Final Report

TO INVESTIGATE THE IMPACT OF PARTICLE SIZE ON MAGNETOELECTRIC (ME) COUPLING OF PRISTINE AND DOPED Z-TYPE HEXAFERRITES SYNTHESIZED BY DIFFERENT ROUTES

UGC Reference No. & Date: F.No. 43-402/2014 (SR) dated 04/09/2015

Submitted to:

University Grants Commission

New Delhi

By

Dr. Rahul Tripathi

Principal Investigator

University Institute of Engineering & Technology

Maharshi Dayanand University, Rohtak

Objectives

- Synthesis of $(Ba,Sr)_3Co_2Fe_{24}O_{41}$ nanoparticles by solid state and sol-gel method followed by ball-milling for particle size reduction.
- Synthesis of Rare earth doped $(Ba,Sr)_3Co_2Fe_{24}O_{41}$ by solid state and sol-gel method followed by ball-milling for particle size reduction.
- To investigate the effect of substitution and particle size on structural parameters of pristine and doped $(Ba,Sr)_3Co_2Fe_{24}O_{41}$ by X-ray diffraction method, SEM, TEM and Rietveld refinement.
- To study the electrical, magnetic, dielectric properties of pristine and doped $(Ba,Sr)_3Co_2Fe_{24}O_{41}$.
- To investigate the effect of particle size on magnetoelectric coupling of pristine and doped $(Ba,Sr)_3Co_2Fe_{24}O_{41}$ by employing different techniques.
- To fabricate thick films of optimized doped $(Ba,Sr)_3Co_2Fe_{24}O_{41}$ by using spin coating technique.

Summary of objectives achieved

- Synthesized $(Ba,Sr)_3Co_2Fe_{24}O_{41}$ and La substituted nanoparticles by solid state and sol-gel method
- Investigated the effect of particle size on the different physical properties of Z-Hexaferrite

Summary/achievement of the work project

The project was sanctioned vide letter F.No. 43-402/2014 (SR) dated 04/09/2015 & the grants for the purpose were received by M. D. University Rohtak in the mid of Nov. 2015 & Nov 2017. Upon receiving the grants various initiatives required for setting up of research facilities were undertaken and the following purchases have been made as per details below:

Equipment Grant: (Total 5.0 lakh)

S. No.	Name of the Equipment	Cost in Rs.	Status
1.	Magnetoelectric measurement unit	4,75,166/-	Supply received payment made
	Total	**4,75,166/-**	

S. No.	Budget Head	Amount Received (Rs.)	Expenditure (Rs.)
1.	**Chemical & Glassware**	2,70,000/-	1,31,122/-
2.	**Contingency**	1,80,000/-	27,608/-
3.	**Overhead**	55,000/-	55,000/-
4.	**Hiring**	25000/-	**nil**
5.	**Travel/Field work**	25000/-	**nil**

As a consequence of the ongoing research activities, **one research paper has been published (re-prints attached), one research is submitted (submitted; copy attached) and one research paper is in process (Draft attached)**. Further, **four papers** in the **conferences** were presented (Details are given at **Annexure-I**). The outcome of the project will be a part of thesis of two research scholars under supervision of one of the collaborators. The following is the work and summary of results obtained so far:

Synthesis techniques with different synthesis conditions

1. Synthesized $Ba_3Co_2Fe_{24}O_{41}$ (BCFO) and $Sr_3Co_2Fe_{24}O_{41}$ (SCFO) via **solid state method** by taking carbonates of Ba/Sr & Co respectively and oxide of iron. The final sintering temperature was varied to optimize the temperature and phase purity of Z-hexaferrites. (Fig. 1). No clear indication of formation of pure Z-Hexaferrite was observed by analyzing XRD patterns (fig.1) instead a mixed phase seems to have produced.

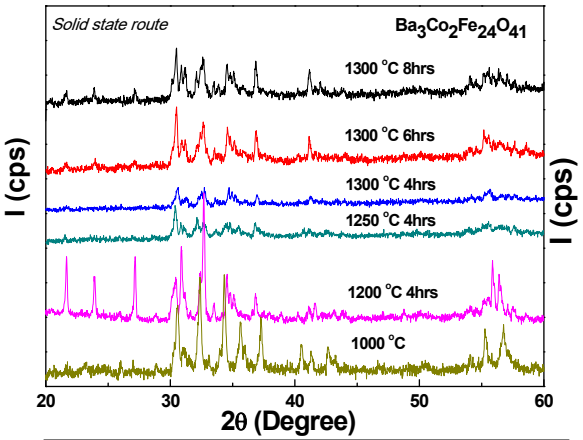

Fig. 1. X-ray diffraction pattern of BCFO; Synthesized by taking carbonates of Ba & Co and oxide of Fe.

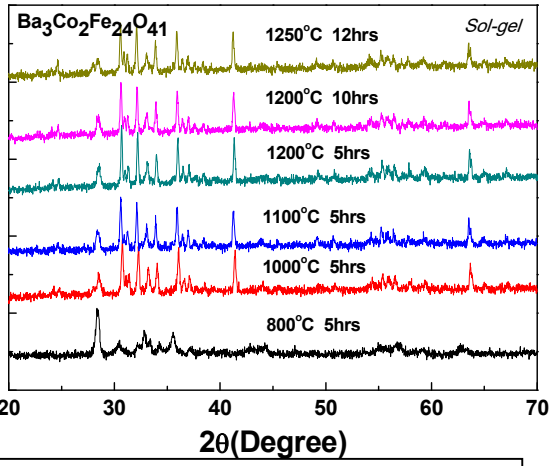

Fig. 2. X-ray diffraction pattern of BCFO; Synthesized by taking carbonates of Ba, nitrate of Co and ferric citrate.

2. Synthesized $Ba_3Co_2Fe_{24}O_{41}$ (BCFO) and $Sr_3Co_2Fe_{24}O_{41}$ (SCFO) via **sol gel method** by taking carbonates of barium/strontium, nitrate of cobalt and ferric citrate respectively (H. Zhang et. al. British ceramic Trans. Vol 102, No.1 (2003)). The figure 2 shows XRD pattern

of BCFO at various sintering temperatures. On further analysis of these pattern using Reitveld analysis and peak fitting (peak fitting results not included), it was concluded that multiple phases were still present in the samples under study and Y- Hexaferrite phase seems more prominent for BCFO. The same was confirmed during refinement of X-ray diffraction data of BCFO whereas refinement of SCFO was done by taking Z-phase during Reitveld refinement. Figure 3 shows a comparative XRD pattern of BCFO samples synthesized at 1250°C and 1270°C respectively and it appears that Z-phase enhanced for the samples sintered at higher temperature i.e.1270°C. Reitveld refinement of both BCFO 1200°C and 1270°C sample is shown in fig. 4. Figure 5 (a) & 5(b) shows the XRD pattern of SCFO 1250°C 12 hrs and its refinement respectively.

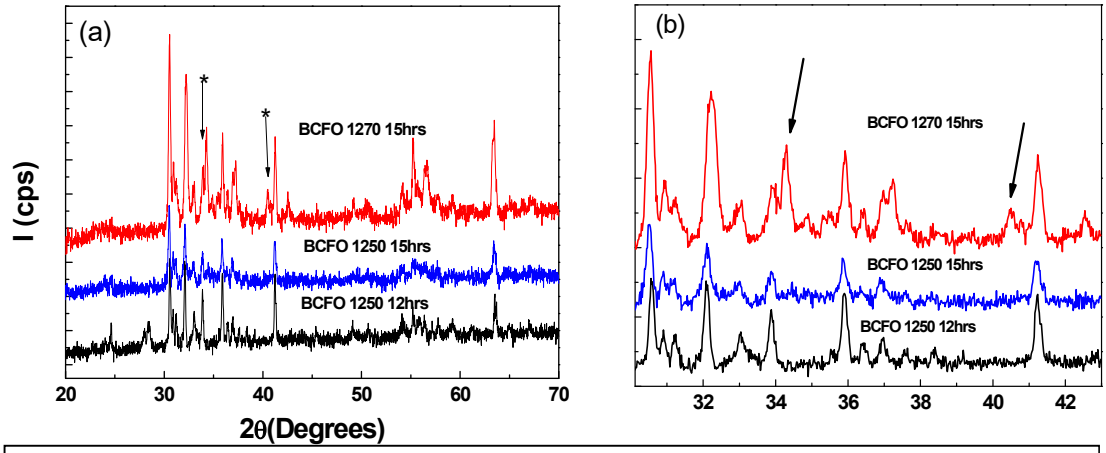

Fig. 3. (a) Comparative XRD pattern of BCFO; (b) Enlarged view of the same.

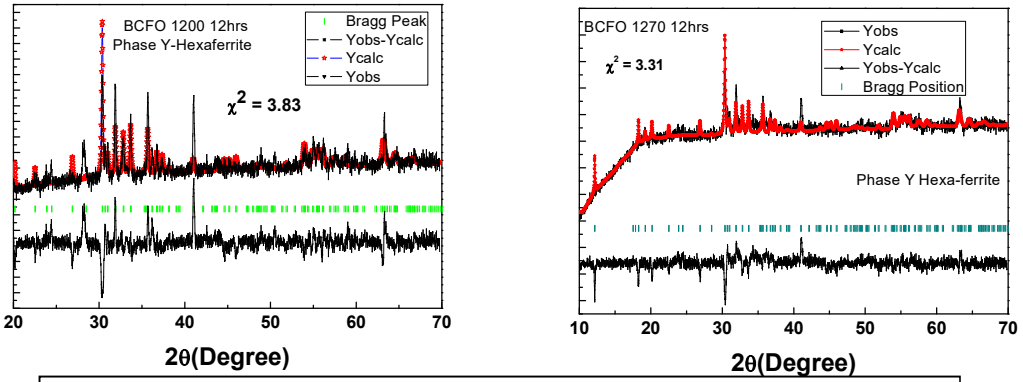

Fig. 4. Reitveld refinement of BCFO at (a) 1200°C and (b) 1270°C

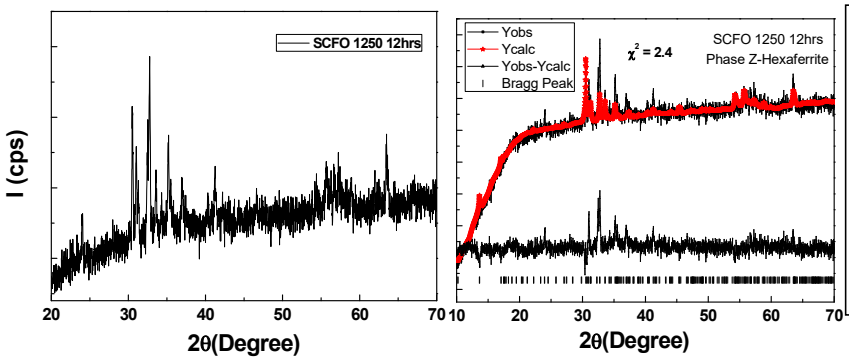

Fig. 5.(a) X-ray diffraction pattern of SCFO and (b) Reitveld refinement of SCFO

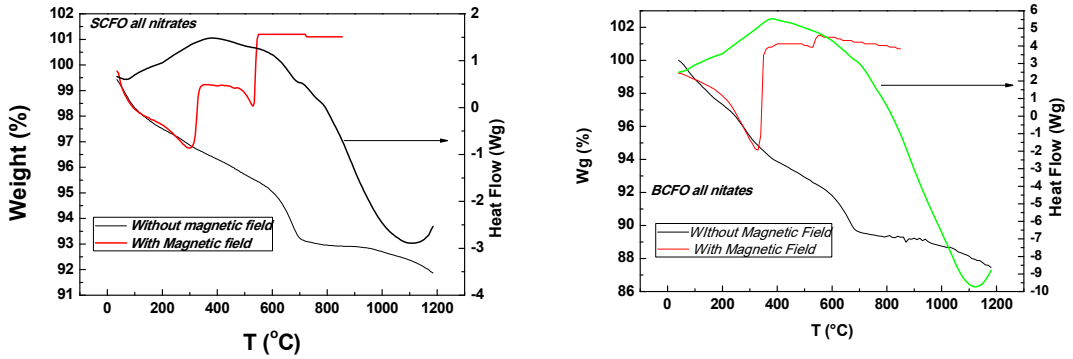

Fig. 6.TGA-DSC plots of (a) SCFO and (b) BCFO

3. Synthesized $Ba_3Co_2Fe_{24}O_{41}$ (BCFO) and $Sr_3Co_2Fe_{24}O_{41}$ (SCFO) via **sol gel method** by taking nitrates of barium/strontium, cobalt and Iron respectively (Sucheta Sharma et. al. Ceramic Int. Vol. 41, Issue 5 7109-7114 (2015)). Further, the detailed analysis of data obtained from BCFO & SCFO and their ball-milled samples prepared using above method is in process and finding will be submitted for publication (Draft enclosed for reference).

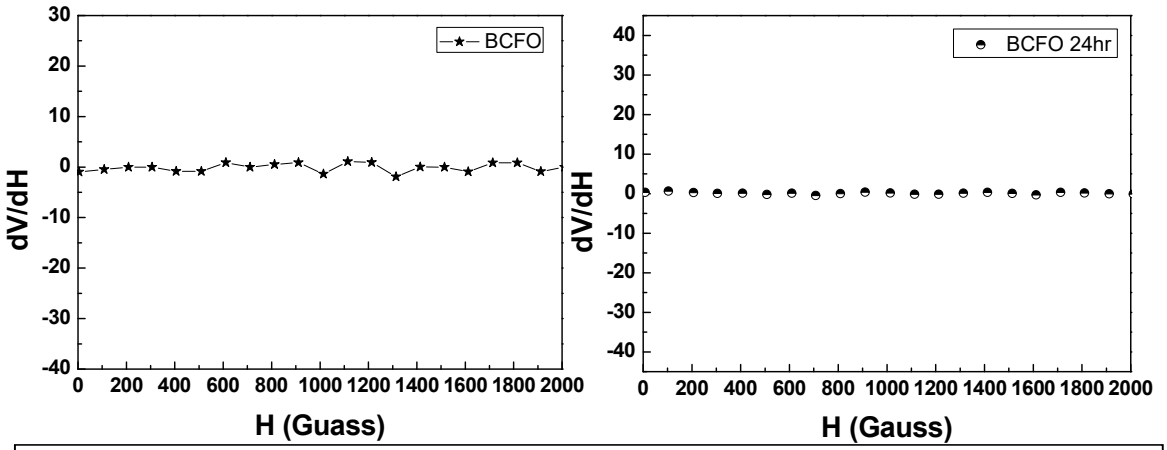

Fig. 7 Room temperature magnetoelectric measurement in terms of change in voltage (V) w.r.t to applied magnetic field (H) for BCFO & SCFO prepared by sol-gel method (point 3)

4. Synthesized $Ba_3Co_2Fe_{24}O_{41}$ (BCFO) and $Sr_3Co_2Fe_{24}O_{41}$ (SCFO) via **solid state method** by taking oxides and carbonates of Co & Fe and Ba/Sr respectively (Y. Kitagawa et. al. Nature mat. ,Vol 9 797-801 (2010)). Figure 8 shows XRD pattern of SCFO calcined at 1000°C for 16 hours and sintered at 1200°C for 16hrs and of BCFO sintered at different temperatures for 16hrs. Again, it seems form fig.8 that mainly Z-hexaferrite phase formed but occurrence of other phases cannot be ruled out totally The TGA-DSC measurements were performed by taking calcined powders were shown in fig. 9.

Further, it is well known that SCFO is synthesized at lower temperature than BCFO. Therefore, detailed investigations were undertaken to analyze the effect of sintering temperature on SCFO along with La-substituted SCFO (Solid State route).

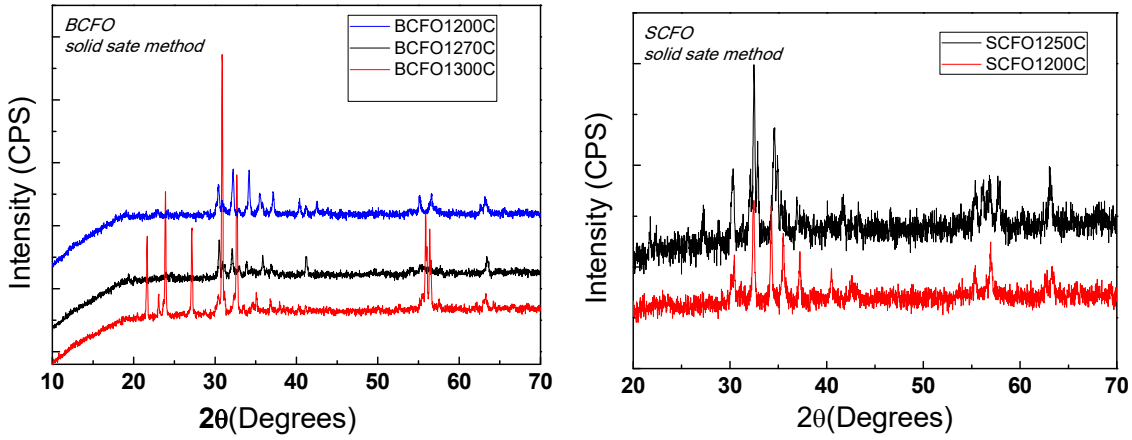

Fig. 8. XRD pattern of BCFO and SCFO synthesized by solid state method by taking carbonates and oxide of Ba/Sr, Fe and Co respectively.

Note: In order to strengthen the optimization of synthesis processes of Z-hexaferrites, studies on Y-hexaferrites as well as M-hexaferrites were also undertaken (figure not included).

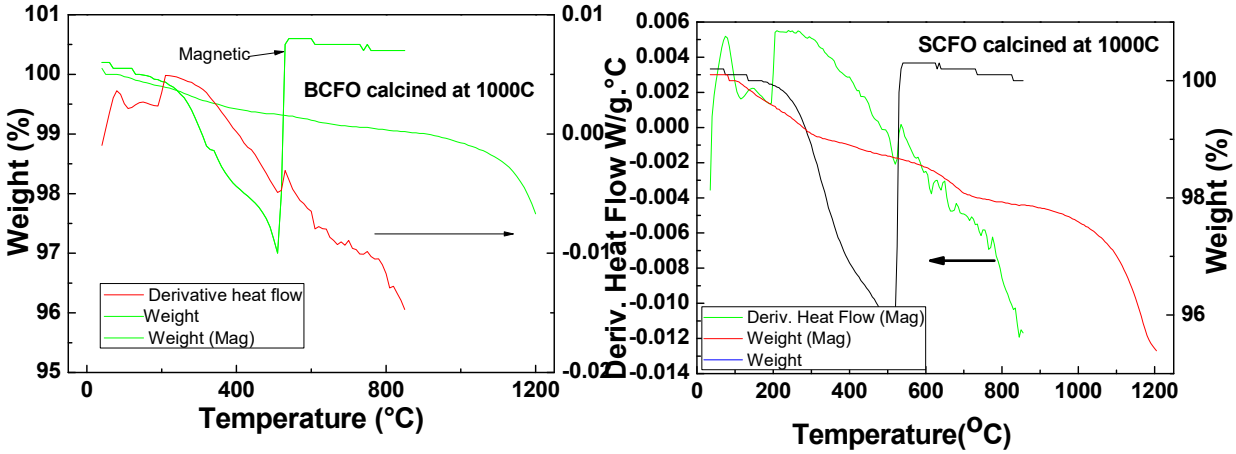

Fig. 9.TGA-DSC plots of (a) SCFO and (b) BCFO powder calcined at 1000°C

5. The La-substituted $Sr_3Co_2Fe_{24}O_{41}$ Z-type Hexaferrites were synthesized using solid state reaction method with starting material Fe_2O_3, $SrCo_3$, La_2O_3 and Co_3O_4 in stoichiometric ratio. All the starting powders were mixed and calcinations at 1000°C for 16 hrs followed by mixing and sintering at 1200°C (Batch-I), 1250°C (Batch-II), 1210°C ((Batch-III) and 1230°C (Batch-IV) for 16hrs cooling rate 60°C/hr up to 900°C followed by natural cooling.

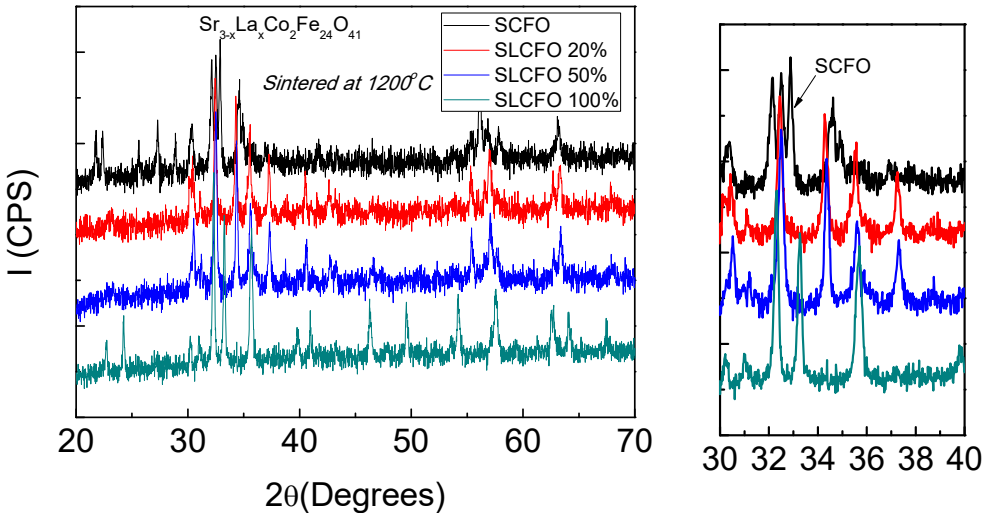

Fig. 10 X-ray diffraction pattern of $Sr_{3-x}La_xCo_2Fe_{24}O_{41}$ for x = 0, 0.6, 1.5 and 3 respectively of Batch-I; Right hand side shows an enlarged portion of same XRD

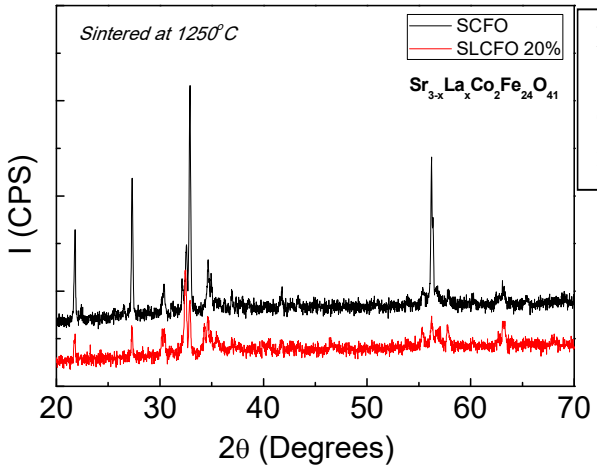

Fig. 11 X-ray diffraction pattern of $Sr_{3-x}La_xCo_2Fe_{24}O_{41}$ for x = 0, and 0.6 sintered at 1250°C for Batch-II respectively.

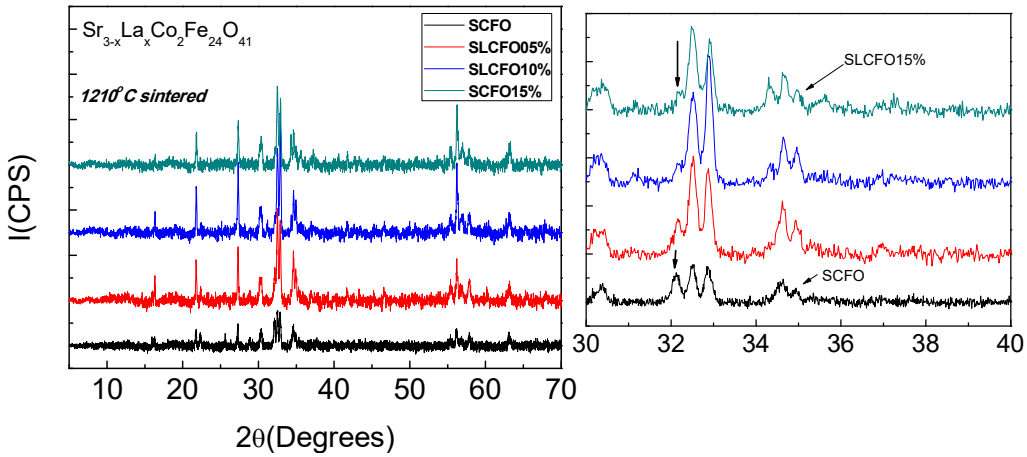

Fig. 12 X-ray diffraction pattern of $Sr_{3-x}La_xCo_2Fe_{24}O_{41}$ for x = 0, 0.15, 0.3 and 0.45 sintered at 1210°C for Batch-III respectively; Right hand side shows an enlarged portion of XRD pattern; Arrow indicates some structural change associated with La substitution.

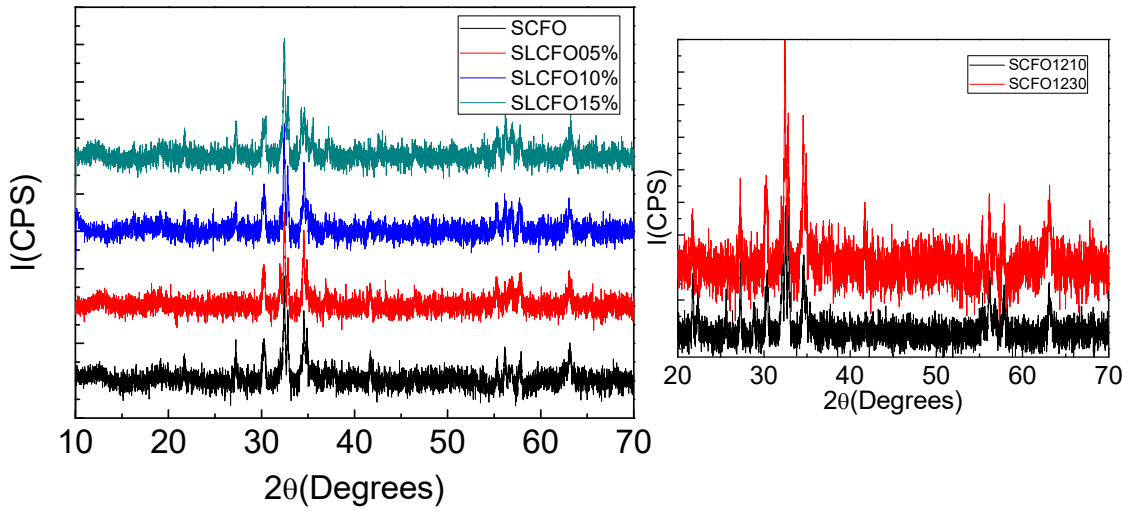

Fig. 13 X-ray diffraction pattern of $Sr_{3-x}La_xCo_2Fe_{24}O_{41}$ for x = 0, 0.15, 0.3 and 0.45 sintered at 1210°C for Batch-IV respectively; Right hand side shows a comparison between SCFO sintered at 1210°C & 1230°C respectively.

The following were the observations and discussions based on synthesis of La-substituted SCFO:

- Batch-I: As shown in fig. 10, major structural changes occurs for substitution of La >20% at Sr-site. Therefore, substitution below 20% seems better to understand the effect of La on SCFO.

- Batch-II: The sintering temperature was raised to 1250°C to improve crystallinity which results in melt like texture of SCFO. Therefore, it was concluded that temperature below 1250°C will be suitable for SCFO. Figure 11 shows XRD pattern of SCFO and La-substituted SCFO.

- Batch-III: The sintering temperature was lowered to 1250°C and as shown in fig. 12, some structural changes seem to occur with La substitution at about 15% in the pristine sample of SCFO sintered. Further, it is clear from these patterns that the value of solubility of La in SCFO without significant change is below 20%.

- Batch-IV: Samples sintered at 1230°C, it is observed that though no major change seems to occur in the samples. Further, on comparing it with Batch-III, no major change was observed, fig. 13.

The field induced room temperature strong ME coupling as observed in Z-type Hexaferrites can be utilized for technical application, therefore, it is quite necessary to

understand the nature of the compound when the particle size is reduced. Further, from physics point of view, it is of great interest to understand the basic principles behind magnetoelectric coupling by substitution at Ca/Sr-site in $(Ba,Sr)_3Co_2Fe_{24}O_{41}$.

Annexure – I

Journal/Articles:

1. Sushma Lather, Anjli Gupta ,Jasvir Dalal, Vivek Verma, **Rahul Tripathi** and Anil Ohlan, "Effect of mechanical milling on Structural, Dielectric and Magnetic properties of $BaTiO_3$– $Ni_{0.5}Co_{0.5}Fe_2O_4$ multiferroic nanocomposites" Ceramics International, 43, 3246–3251(2017).
2. Sushma Lather, Jasvir Dalal, Anjli Gupta, Sukhbir Singh, D. P. Singh, Sajjan, **Rahul Tripathi** and Anil Ohlan "Effect of mechanical milling on the structural, Dielectric and Magnetic properties of PbTiO3 –$Ni_{0.5}Co_{0.5}Fe_2O_4$ multiferroic nanocomposites" submitted in Ceramic international
3. Effect of particle/grain size on magnetic, dielectric and magnetoelectric properties of Z- type $(Ba, Sr)_3Co_2Fe_{24}O_{41}$ Hexaferrite (in process)

Papers in Conferences/Seminar/Symposium

1. Effect of mechanical milling on dielectric, ferroelectric and magnetic properties of Z-type hexaferrite $Ba_3Co_2Fe_{24}O_{41}$
   Sushma Lather, Anjli Gupta, Jasvir Dalal, **Rahul Tripathi** and Anil Ohlan

   Presented by Sushma Lather at First international conference on Novel Approaches in Science Engineering & Technology (NASET 2017) organized by Madhav University, Pindwara, Sirohi (Rajasthan) from 24-25 Feb 2017.
2. Dielectric, Ferroelectric and Magnetic properties of Z–Type hexaferrite $Sr_3Co_2Fe_{24}O_{41}$ with effect of mechanical milling
   Sushma Lather, Anjli Gupta, Jasvir Dalal, **Rahul Tripathi**, Sajjan Dahiya, A.S.Maan and Anil Ohlan

   Presented by Sushma Lather at International Conference on Advances in Analytical Science (ICAAS-2018) organized by CSIR-IIP, Dehradun from 15-17 March 2018
3. X-ray diffraction study of La substituted strontium (Sr) based Z-Hexaferrite
   Sukhbir Singh, Sajjan, Anil Ohlan, **Rahul Tripathi** and A.S. Maan

   Presented by Sukhbir Singh at International Conference on Advances in Analytical Science (ICAAS-2018) organized by CSIR-IIP, Dehradun from 15-17 March 2018
4. Z-type Co-Hexaferrites: an analysis of synthesis parameter
   Rahul Tripathi, Sukhbir Singh, Sushma Lather, Jasvir Dalal and Anil Ohlan

   Presented by Rahul Tripathi at National Seminar on Recent Trends in Science & Technology: A Computational Approech (RTSTCA 2018) organised by Ch. Bansi Lal University, Bhiwani on 22 March 2018.

PhD students:

Yes; Outcome of the project will be a part of thesis of two PhD students of a collaborator.

Ceramics International 43 (2017) 3246–3251

Contents lists available at ScienceDirect

Ceramics International

journal homepage: www.elsevier.com/locate/ceramint

Effect of mechanical milling on structural, dielectric and magnetic properties of $BaTiO_3$–$Ni_{0.5}Co_{0.5}Fe_2O_4$ multiferroic nanocomposites

Sushma Lather[a], Anjli Gupta[a], Jasvir Dalal[a], Vivek Verma[b], Rahul Tripathi[c,*], Anil Ohlan[a]

[a] Department of Physics, Maharshi Dayanand University, Rohtak 124001, India
[b] Department of Physics, Hindu College, University of Delhi, Delhi 110007, India
[c] University Institute of Engineering & Technology, Maharshi Dayanand University, Rohtak 124001, India

ARTICLE INFO

Keywords:
Nanocomposites
Multiferroics
Dielectric properties
Magnetic properties
Ball-milling

ABSTRACT

The coexistence of ferroelectricity and ferromagnetism has triggered great interest in multiferroic materials. Multiferroic with strong room temperature magnetoelectric (ME) coupling can provide a platform for future technologies. In this paper, we have investigated the effect of mechanical milling on the properties of multiferroic nanocomposites synthesized by mixing barium titanate ($BaTiO_3$) (BT) and nickel cobalt ferrite ($Ni_{0.5}Co_{0.5}Fe_2O_4$) (NCF). This process has resulted into reliable disposal of a given quantity of NCF nanoparticles in BT grid and composite samples of different particle sizes (< 500 nm) have been obtained by varying the duration of ball-milling for 12, 24, and 48 h. The presence of NCF within BT powder has been confirmed by X-ray Diffraction (XRD) and magnetization measurements (MH). Structural analysis was performed by using Reitveld refinement method that shows that the tetragonality of $BaTiO_3$ structure get reduced in submicron range. Variations in ferroelectric and dielectric properties with reduction in particle size/milling duration have been studied by P-E loop tracer and Impedance analyzer. The dielectric constant value of 400 has been observed for BT-NCF0 that increases to 9.7 K for composite sample ball mill at 48 h whereas remnant polarization increases to 4.2 μC/cm^2. These composites with high dielectric constant that changes with temperature and particles size find application in energy storage devices, sensor and memory devices.

1. Introduction

Magnetism and electricity together forms the basis of world's most advanced technologies. Materials possessing these properties have been studied extensively so as to tailor these properties for application purposes. Over last few years, efforts have been put together to discuss a group of materials known as multiferroics which is generally defined as a material possessing two or more ferroic orders (like ferromagnetism, ferroelectricity, ferroelasticity). The coexistence of these ferroic orders in a single compound with strong coupling between them has huge potential for practical application especially in the field of memory devices [1–4]. Among multiferroics, material with strong coupling of ferromagnetic and ferroelectric property is of great interest as it can provide control of magnetism through electric field and vice-versa. Generally, it has been observed that these two order parameters are mutually exclusive and strong magnetoelectric (ME) coupling between these order parameters together in a single compound is difficult to obtain [5–9]. Moreover, for practical purpose, room temperature strong ME coupling is required. Therefore, composites/laminate which consists of ferroelectric and ferromagnetic phases/layers serves as a better option to obtain strong ME coupling at room temperature [10–13]. Reasonably high values of ME coefficient were observed [14] for such composites/laminate structures. These engineered multiferroic material/structure can provide an edge over single phase material as they are easy to synthesis and strong coupling could be achieved at room temperature. Among these multiferroic materials, a composite consists of $BaTiO_3$ and $PbTiO_3$ as ferroelectric phase and $CoFe_2O_4$ as ferromagnetic phase were extensively studied [15–17]. Recently, it has been found that the coercivity of cobalt ferrite increase by substitution of metal ions for Co and Fe in cobalt ferrite. Pulišová et. al.[18] has compared the properties of $CoFe_2O_4$, $Ni_{0.5}Co_{0.5}Fe_2O_4$ and $NiFe_2O_4$ whereas Saffari et al. [19] has investigated the effect of Fe substitution with Cr in $Co_{0.5}Ni_{0.5}Cr_xFe_{2-x}O_4$ nanoparticles. They have reported the increase in coercivity and decrease in saturation magnetization with the substitution. The reduction in coercivity results from the decrease in anisotropy that will be necessary for strong magnetostatic interactions [20,21]. For applications, it is always advantageous to use lead free compound, therefore, $BaTiO_3$ composites drew special attention. ME coefficient (α_{ME}) as high as 135 mV/cm Oe was obtained for $BaTiO_3$-$CoFe_2O_4$ laminates structure [22] and 8130 μV/cm Oe for

* Corresponding author.
E-mail address: rtrnpl@gmail.com (R. Tripathi).

http://dx.doi.org/10.1016/j.ceramint.2016.11.152
Received 24 July 2016; Received in revised form 3 November 2016; Accepted 22 November 2016
Available online 23 November 2016

$BaTiO_3$-$CoFe_2O_4$ core-shell structure [23].

Walther et al. [11] {*(1-x)BaTiO$_3$- x CoFe$_2$O$_4$*} with x=0.1, 0.2, 0.3, 0.4, 0.5 has achieved the optimization for 60:40 whereas Zhang et al. [24] have studied the effect of concentration for similar composite {*(1-x)BaTiO$_3$- x Ni$_{0.5}$Zn$_{0.5}$Fe$_2$O$_4$*} by taking x=0.2, 0.5 and 0.8 and achieved optimized results for x=0.8. Many other research groups have also studied the effect of change in ratio of ferroelectric to ferromagnetic concentration. Motivated by these studies and availability of very few reports, we have synthesized $BaTiO_3$ (BT)-$Ni_{0.5}Co_{0.5}Fe_2O_4$ (NCF) composite in 80:20 and discussed the effect of mechanical milling (particle/grain size) on its properties. These composites consist of ferroelectric BT phase and ferromagnetic NCF phase. In such composites ferroelectric phase interact via strain to ferromagnetic phase and therefore behaves like multiferroics. BT being a good piezoelectric material and NCF exhibits magnetostriction. Since these strain fields propagates through phase boundaries, hence, it is very important to analyze the effect of grain boundaries in such composites. It is well known that the piezoelectric and ferroelectric properties of $BaTiO_3$ attain highest values at ~1 μm grain size [25], so it is interesting to discuss BT composites in submicron range. Therefore, present works systematically discuss the effect of grain size on the structural, dielectric, ferroelectric and magnetic properties of $BaTiO_3$-$Ni_{0.5}Co_{0.5}Fe_2O_4$ nanocomposites. The variation in particle/grain size of composites was achieved by ball-milling.

2. Experimental

$BaTiO_3$ was synthesized by using conventional solid state reaction method from fine powder of $BaCO_3$ (99.9%) and TiO_2 (99.9%). These powders were mixed in appropriate ratio and ball milled for 3 h. The mixed powder was calcined at 1100 °C for 1.5 h. $Ni_{0.5}Co_{0.5}Fe_2O_4$ was synthesized by using precursor method from $Ni(NO_3)_2{\cdot}6H_2O$, $Co(NO_3)_2{\cdot}6H_2O$ and $Fe(NO_3)_3{\cdot}9H_2O$. The stoichiometric ratio of these nitrates was dissolved in double distilled water. Citric acid was added to the solution under constant stirring. In order to maintain the pH of the solution at 8.0, ammonium hydroxide was added drop wise. The solution was evaporated and dried by placing it on a magnetic stirrer (90 °C) under continuous stirring to form a viscous gel. Subsequently, the gel so formed was dried at 100 °C until it ignited in air. With nitrates as oxidant and citric acid as reductant, the gel was burnt to form dendrite structure which was then grounded in a pestle mortar. The precursor consisting of oxides and carbonates were calcined at 1000 °C for 2 h resulting to form nickel cobalt ferrite ($Ni_{0.5}Co_{0.5}Fe_2O_4$).

In order to reduce the size of both BT and NCF, the as synthesized materials were ball milled separately for different duration i.e. 12, 24 and 48 h in planetary ball mill and nanocomposites $BaTiO_3$-$Ni_{0.5}Co_{0.5}Fe_2O_4$ [BT-NCF] were prepared by mixing powdered BT and NCF in 80:20 wt ratio. Depending upon the duration of ball milling, the composites were named as BT-NCF1, BT-NCF2 and BT-NCF3 corresponding to 12, 24 & 48 h milling time. The complete synthesis process was illustrated in Fig. 1. The pellets were formed with pressure of 10 ton using hydraulic press. Polyvinyl alcohol (PVA) was used as a binder. In order maintain the particle size, final sintering of all pellets was done at 900 °C for 2 h to form the fully dense nanocomposites ceramics. The phase structure of the BT-NCF composite samples was investigated by X-ray diffractometer (XRD) with CuK_α radiation (Rigaku Miniflex, 600). Grain structure and morphology was studied by using scanning electron microscope (SEM) (su8010, Hitachi). The room temperature dielectric/loss spectra of the BT-NCF composite ceramics were recorded using the multifunctional impedance analyzer (Wayen-Kerr 6500B) from 100 Hz to 10 MHz. Ferroelectric measurements were performed by using P-E loop tracer (Marine India ltd). Magnetic measurements were performed on quantum core MPMS.

3. Result and discussion

As shown in Fig. 2 all the samples of $BaTiO_3$ crystallizes in tetragonal structure (*P*4*mm*). Further, it is observed that the intensity of XRD peaks decreases and broadening of peak occurs for the samples with higher milling period. This clearly suggests that the particle size reduces with ball-milling (Fig. 2). Similar observations were made for $Ni_{0.5}Co_{0.5}Fe_2O_4$ (spinel cubic structure) (JCPS Card 74–2081). Although some peaks around 2θ =29 ° (marked as '*') was observed for as-synthesized BT but they does not corresponds to $BaCO_3$. This observed peak (2θ =29°) in the XRD pattern for as synthesized BT sample can be attributed to the presence of $Ti_nO_{2\ n-1}$ phases [26]. Interestingly, with mechanical milling (i.e. 12, 24 & 48 h), the peaks around 2θ =29° reduces and that of $BaCO_3$ appears (marked as '#'). The intensity of $BaCO_3$ peak seems increasing with the milling hours; it is highest for 48 h BT ($BaTiO_3$) sample whereas it is nearly absent for BT sample. Moreover, only the milling time is different for samples under present study, therefore, this difference in XRD pattern may arise from ball-milling and the possible explanation for occurrence of $BaCO_3$ peaks can be linked with the use of tungsten carbide balls or with methanol used during milling process [27]. Since the process of ball-milling involves mechanical crushing of the powder therefore, in such process carbon may have reacted to form $BaCO_3$ phase [27]. The presence of $BaCO_3$ was further confirmed by Rietveld refinement (Fullprof) of the X-ray diffraction pattern.

Fig. 3 shows the fitted XRD pattern of BT 48 h sample, here, refinement was performed by taking two phases (i.e. $BaTiO_3$ & $BaCO_3$) and better fitting was observed by taking two phase model (χ^2=3.83). Arlt et.al. [28] had mentioned that with decrease in the grain size the tetragonality of the samples decreases as (c/a-1) < 1% and attain a pseudo-cubic structure with c/a~1. Decrease in tetragonality of $BaTiO_3$ represents poor ferroelectric behavior. The lattice parameters corresponding to as synthesized BT and BT 48 h are listed in Table 1. At most care has been taken during refinement so as to keep minimum thermal factors [29] so that the variation of lattice parameters can be analyzed. The c/a ratio seems to be unity for all BT samples. The reduction in tetragonality of the structure was further confirmed by analyzing the splitting of peaks (200) and (002) and it was found that instead of clear splitted peaks corresponding to tetragonal structure a kind of overlapping was observed for all samples. From above discussion it is clear that with reduction in particle size (Ball-milling) of $BaTiO_3$, tertragonal structure of BT destabilized and results in some sort of pseudo-cubic structure. Further, there are several reports [30–33] on the structural studies of BT nano-particles. Ram et. al. [33] has mentioned that nanoparticles of BT can have orthorhombic structure and on the other hand, Yashima et. al. [31] observed hexagonal & tetragonal mixed phase for BT nanoparticles. In present case, all the samples were refined using *P*4mm space group of tetragonal structure.

Fig. 4 shows the XRD pattern of BT-NCF samples. The percentage of ferrite phase is low, therefore, high intensity XRD peaks corresponds to BT phase [34]. Composites contains no peak/(s) corresponding to inter-diffusion of two phases at grain boundaries as reported by Ghosh et. al. [34] and thus all the properties of given composites can be analyzed and explained by taking two pure phases i.e. BT and NCF.

Fig. 5 shows the scanning electron micrographs of BT-NCF composites. It is clearly seen from these SEM images that the average grain size of all the samples under present study is less than 500 nm. This implies that all the BT-NCF composites are in sub-micron range. The particles become more round in shape for BT-NCF 48 h. On comparing the SEM images of BT-NCF with that of 48 h ball-milled sample, it was observed that the average grain size reduces for longer milling period. Since the particle size of all the samples is in nano-range, therefore, surface morphology as perceived from SEM images does not indicate high sample density. However, from density measurements of these samples, it is confirmed that the density of all the samples are of same order.

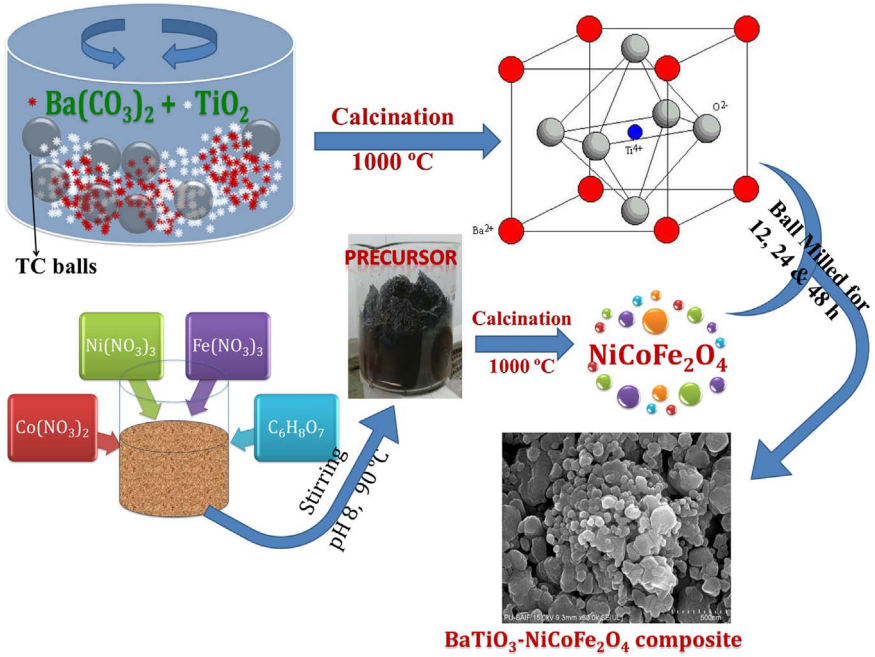

Fig. 1. Schematic illustration for the synthesis of $BaTiO_3$-$Ni_{0.5}Co_{0.5}Fe_2O_4$.

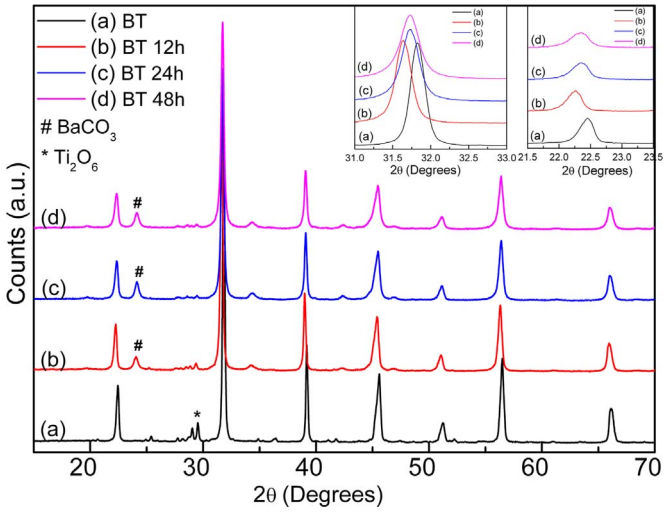

Fig. 2. X-ray diffraction pattern of $BaTiO_3$ and Ball-milled $BaTiO_3$ (12, 24 & 48 h) whereas inset shows the enlarged view of the peaks at 2θ =22° and 32°.

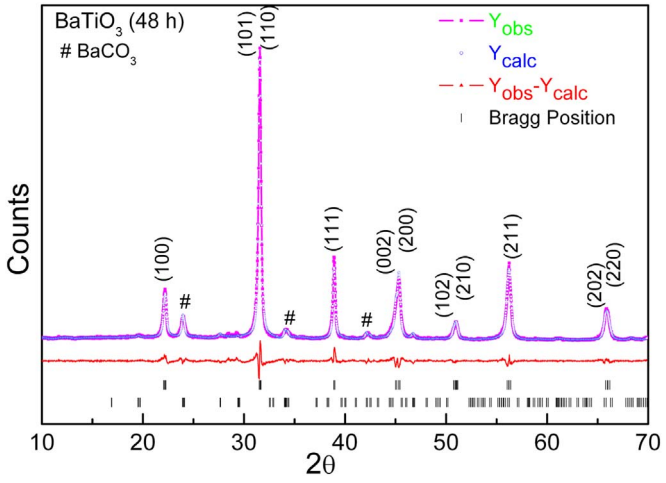

Fig. 3. Rietveld refined X-ray diffraction pattern of $BaTiO_3$ (48 h); # indicates the $BaCO_3$ phase.

Table 1
Lattice parameters of $BaTiO_3$ samples.

$BaTiO_3$	a (Å)	b (Å)	c (Å)	c/a
Pristine	4.007	4.007	4.0232	1.004
48 h	3.999	3.999	4.0253	1.006

The variation of dielectric constant and dielectric loss with temperature of composite samples is shown in Fig. 6. Composite sample of 24 h possess a diffused but recognized transition temperature (para-electric-ferroelectric phase transition) at 129 °C while more flattened and broad transition were observed for other composite samples (Fig. 6a). Similar observations were reported by Ghosh et. al. [34] for nanocrystalline $BaTiO_3$ composites. The reason of such flattened peaks can be associated with submicron size of the composite material. Since the transition is broad, therefore in the present case the effect of grain size reduction on the transition temperature cannot be examined with certainty. However, very recently, Wang et.al. [32] has mentioned that good dielectric behavior can be observed even with 8 nm particle prepared by two step method.

Further, the dielectric constant increases towards high temperature range for all composites samples. Fig. 6b shows the variation of dielectric losses with temperature and it is observed from these curves that the dielectric loss decreases as temperature increases, attain a certain lowest value and then again increases with temperature. Overall, relatively low dielectric losses were observed for the BT-NCF samples. The low dielectric loss is due to high resistive BT and NCF phases [35]. However, Verma et. al. [9] reported the Pr doped multi-ferroics bismuth ferrites having high dielectric loss and Zhang et al. [24] stated that (1-x) $BaTiO_3$- $xNi_{0.5}Zn_{0.5}Fe_2O_4$composite samples with higher concentration of ferromagnetic part are lossy in nature, The variation of dielectric constant with frequency for BT-NCF composites samples is shown in Fig. 7 and it is observed that the dielectric constants of composites decrease with the frequency. Moreover, the dielectric constant decreases sharply at low frequencies for BT-NCF2 & BT-NCF3 samples and attains a constant value at higher frequencies. As we know that in the presence of alternating field,

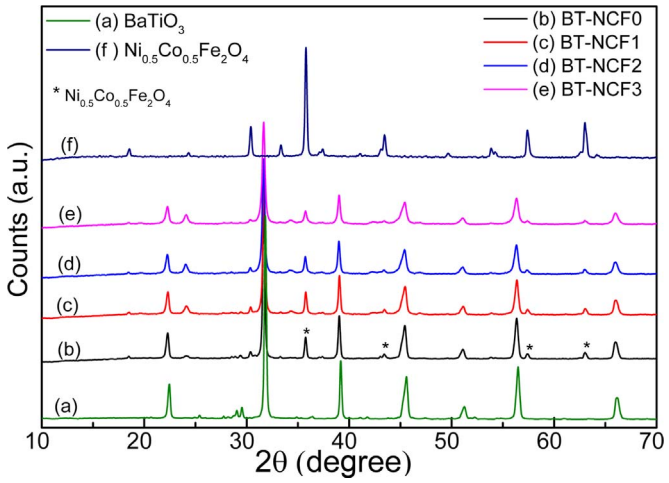

Fig. 4. X-ray diffraction pattern of $BaTiO_3$, $Ni_{0.5}Co_{0.5}Fe_2O_4$ and BT-NCF composites ball-milled for 0 h, 12 h, 24 h and 48 h.

the direction of polarization changes and dipoles try to align with the applied field. Therefore, some time is required for rotation of dipoles or movement of charges known as relaxation time (ς). If the frequency of the applied field is greater than the 1/ς, the direction of polarization is not able to remain align with the field and thus discontinued to contribute towards the total polarization. Similarly, for ionic and electronic polarization, with the increase in frequencies, the movement of charge cannot sustain with the alternating field and discontinued to contribute towards the total polarization. Thus, with the increase in frequency, the net polarization falls and hence its dielectric constant decreases. Interestingly, the low frequency dielectric constant increases with reduction in size and this frequency behavior of BT-NCF samples can be attributed to Maxwell-Wagner type interfacial space polarization [35,36]. The sample with increased ball-milling period possesses smaller grain size, therefore, number of grain boundaries increases for 24 h & 48 h milled sample and thus enhances the space charge polarization. In case of identical dielectrics, the charge density is zero but various studies have shown that charge is trapped at the physical interface of two identical materials due to different degree macro, micro and nano imperfections, a discontinuity in the dissemination of trapping sites has been created. While in composite materials (heterogeneous), finite charge density exists at the interface. The discontinuity in conductivity/permittivity forms space charge at the interface which is considerably different from space charge accumulation due to charge transport [37,38]. As the grain size decrease more and more interface boundaries build-up that contributes to the increase space charge density and hence the dielectric constant of the composite material [39]. At low frequency, dielectric constant of BT-NCF0 composite sample is 400 which is smaller as compared to Zhang et al.[24] whereas for BT-NCF2 and BT-NCF3 it increases to 8.8 k and 9.7 k respectively. However, at higher frequencies dielectric constant is constant for all the samples.

Fig. 8 shows polarization versus electric field (*p*-E) loops of all composite i.e. BT-NCF0, BT-NCF1, BT-NCF2, BT-NCF3 & pure $BaTiO_3$ (for comparison). Unlike the sigmoid shape of P-E loops as reported by Tan et. al. [39], in present case unsaturated P-E loops was observed. Mao et. al. [40] in their study on $BaTiO_3$-PVDF composites had observed enhanced ferroelectric properties with increasing size of $BaTiO_3$ particle. With ferrite composition, small increase in saturation polarization (P_s) and remnant polarization (P_r) has been observed as compared to $BaTiO_3$. The maximum Pr value of 5.7 μC/cm^2 and Ps value of 8.4 μC/cm^2 has been recorded for BT-NCF1 sample. However,

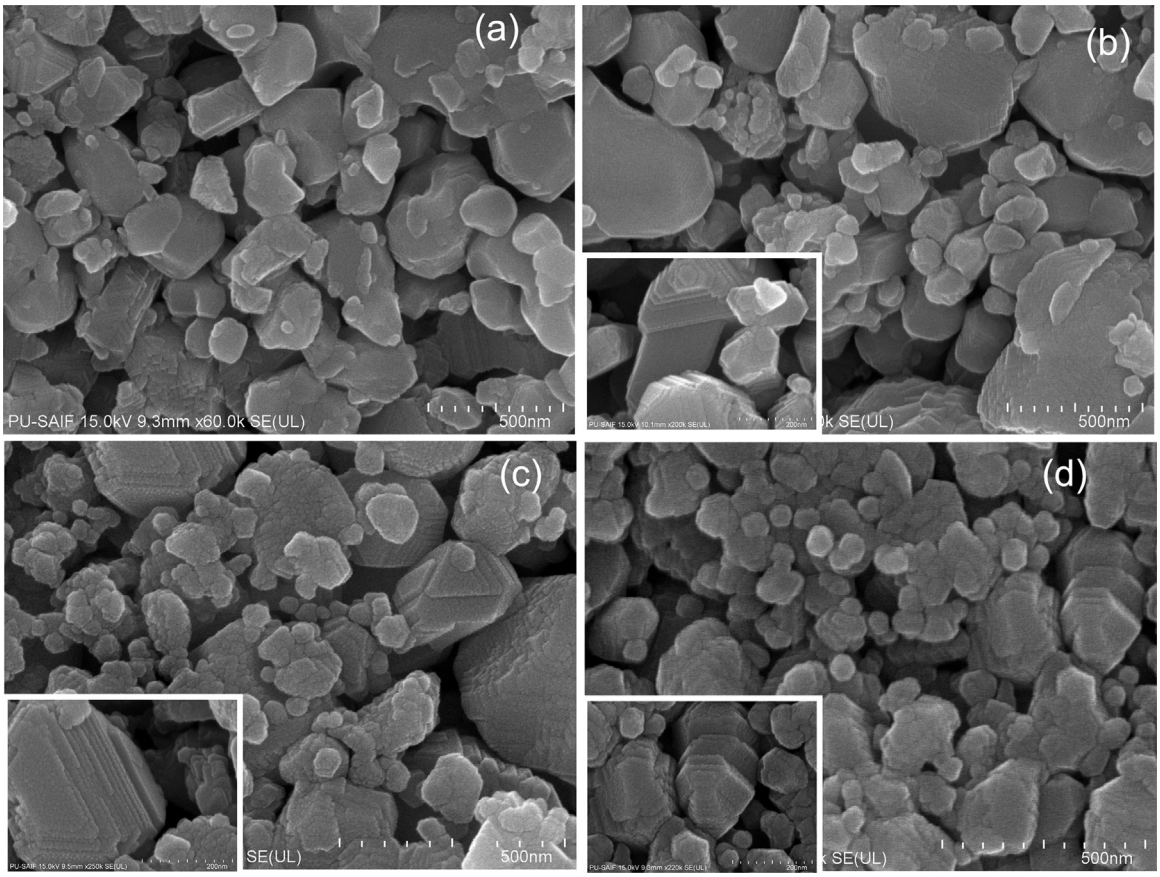

Fig. 5. (a) SEM image of as synthesized (a) BT-NCF0, (b) BT-NCF1, (c) BT-NCF2, and (d) BT-NCF3composites ball-milled for 0 h, 12 h, 24 h and 48 h. Whereas, the inset shows the SEM images of the respective samples at higher resolution.

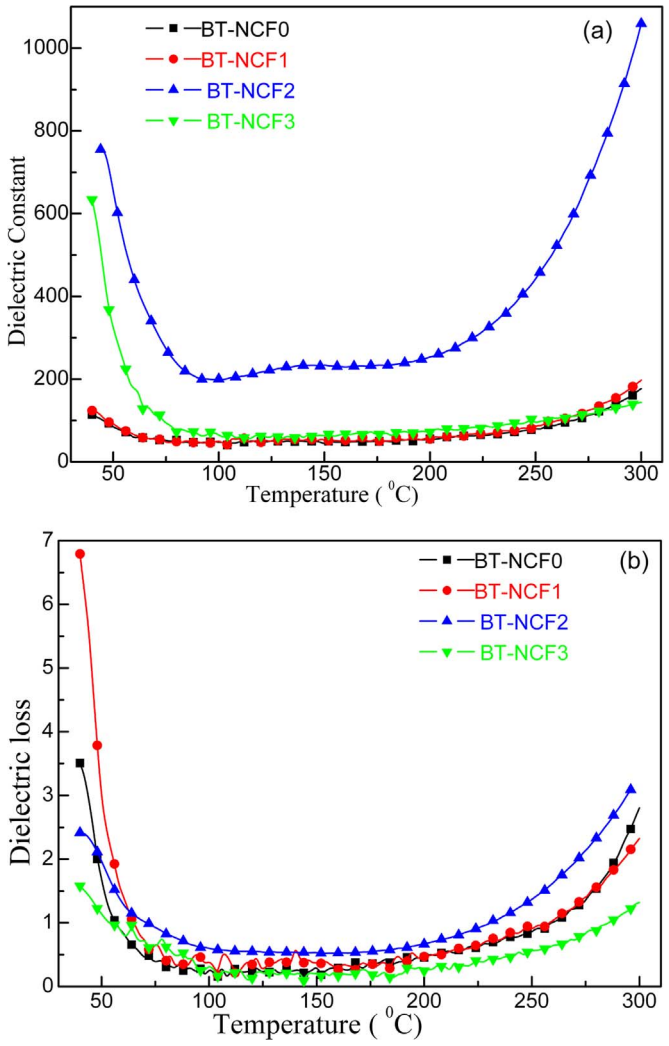

Fig. 6. Variation of (a) dielectric constant and (b) dielectric loss with temperature of BT-NCF composite samples (frequency =1000 Hz.).

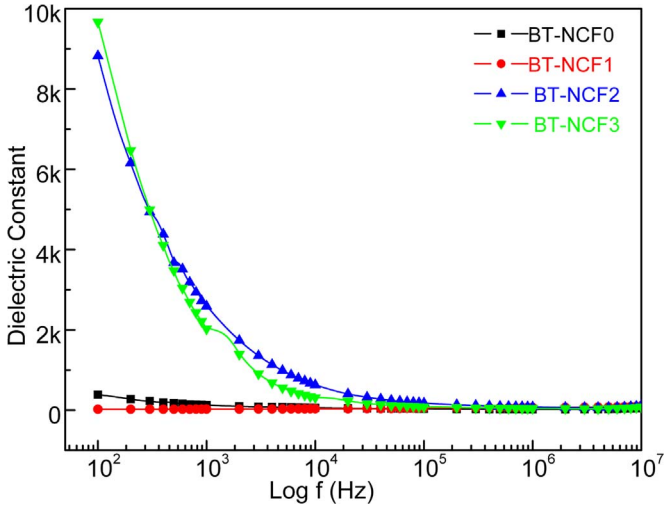

Fig. 7. Variation of dielectric constant with frequency of BT-NCF composite samples at room temperature.

lossy or non-ferroelectric behavior was recorded for BT-NCF2 and BT-NCF3 [41]. The P-E loops corresponding to pure $BaTiO_3$ and BT-NCF0 nearly overlap, therefore, presence of ferrite phase does not seems responsible for the variation of ferroelectric behavior of composite

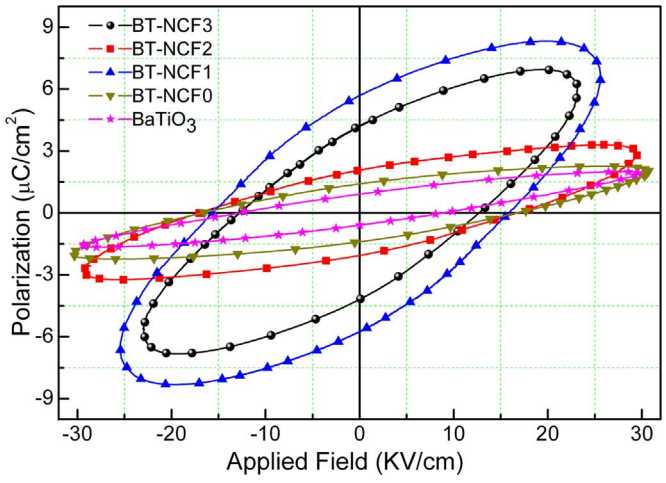

Fig. 8. Room temperature P-E loops of $BaTiO_3$ and BT-NCF composites.

samples. Further, it should also be noted that the percentage of NCF is low compared with that of BT phase. This infers that modifications in the ferroelectric behavior of the composite sample are due to reduction in the particle size of the composites [42] and the same can be correlated with decrease in the tetragonality of the samples (c/a→1) with increasing Ball-milling (as discussed during XRD analysis) [43]. As discussed in previous section, SEM images confirmed that the particle size of all the composites samples lies within submicron range, consequently, porosity/density of the samples can play their role in the observed dielectric and ferroelectric behavior of the material. But, all the samples under present study seems to have similar surface porosity/density, therefore, it does not appear to be the reason for the observed variation in dielectric and ferroelectric of the samples.

Magnetization measurements of BT-NCF composites (*m*-H) are shown in Fig. 9. Even though the present composition contains small amount of ferrite phase, yet excellent values of saturation magnetization and coercivity were recorded. In ferrite, usually it is observed that with decrease in the particle size there is an obvious [44,45] decrease in saturation magnetization (M_s). Similar observations were made on BT-NCF samples except for BT-NCF3 sample where saturation magnetization increases as compared with that of other BT-NCF composites. M_s as high as 10.8, 9.7, 6.5 and 12.9 emu/g were observed for BT-NCF0, BT-NCF1, BT-NCF2 and BT-NCF3 respectively. The inset of Fig. 9 is showing an enlarged portion of M-H curves, BT-NCF3 sample shows maximum coercivity (H_c) as compared with others; H_c is 340, 412, 400

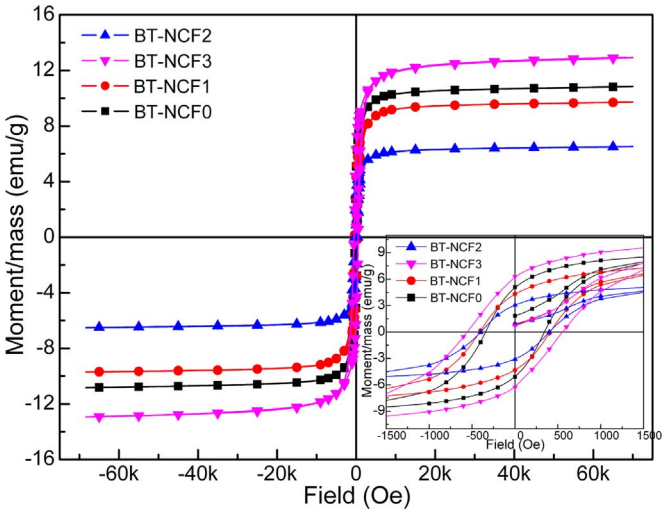

Fig. 9. Room-temperature ferromagnetic hysteresis loops of BT-NCF composite samples whereas Inset shows enlarged portion of M-H curves at lower applied field.

and 556Oe for BT-NCF0, BT-NCF1, BT-NCF2 and BT-NCF3 respectively [46].

4. Conclusion

The multiferroic composite of $BaTiO_3$-$Ni_{0.5}Co_{0.5}Fe_2O_4$ was prepared by conventional methods. Samples were ball-milled for different durations (12, 24 & 48 h) to reduce the particle size of the constituent phases of the composite. The effect of size reduction was clearly visible in X-ray diffraction patterns. The value c/a ratio of $BaTiO_3$ phase confirms the fact that the tetragonality of the structure which is responsible for ferroelectric behavior weakens for smaller grain size. Frequency dependent dielectric constant for BT-NCF2 and BT-NCF3 exhibits sharp change at low frequency which may be due increased grain boundary density results in enhanced space charge polarization (Maxwell-Wigner type). The effect of ferrite phase on the properties of $BaTiO_3$ seems negligible. It is advisable to have optimum grain size of $BaTiO_3$ based multiferroic composites so that strong ME coupling could be achieved which is a very important parameter for practical applications.

Acknowledgement

We would like to acknowledge CIF Punjab university of SEM measurements. We are also like to thanks DST, New Delhi and UGC, New Delhi for providing financial support under DST-FIST scheme (SR/FST/PSI-162/2011) and UGC-SAP {F530/5/DRS/2012(SAP-1)}, respectively. One of the authors RT would like to thank UGC-India for providing financial support under UGC-MRP ((F. No. 43–402/2014(SR)).

References

[1] S.-W. Cheong, M. Mostovoy, Multiferroics: a magnetic twist for ferroelectricity, Nat. Mater. 6 (2007) 13–20.
[2] S. Dong, J.-M. Liu, S.-W. Cheong, Z. Ren, Multiferroic materials and magnetoelectric physics: symmetry, entanglement, excitation, and topology, Adv. Phys. 64 (2015) 519–626.
[3] Y. Han, Z. Zhang, F. Wang, W. Mi, K. Zhang, Fabrication and characterization of a magnetoelectric memory cell of 50Ba $(Zr_{0.2}Ti_{0.8})O_3$–$50Ba_{0.7}Ca_{0.3}TiO_3$/$Fe_{70}Ga_{30}$, Mater. Lett. 170 (2016) 192–195.
[4] Z. Zhou, B.M. Howe, M. Liu, T. Nan, X. Chen, K. Mahalingam, N.X. Sun, G.J. Brown, Interfacial charge-mediated non-volatile magnetoelectric coupling in $Co_{0.3}Fe_{0.7}$/$Ba_{0.6}Sr_{0.4}TiO_3$/Nb:$SrTiO_3$ multiferroicheterostructures, Sci. Rep. 5 (2015).
[5] K. Wang, J.-M. Liu, Z. Ren, Multiferroicity: the coupling between magnetic and polarization orders, Adv. Phys. 58 (2009) 321–448.
[6] M. Matsubara, S. Manz, M. Mochizuki, T. Kubacka, A. Iyama, N. Aliouane, T. Kimura, S.L. Johnson, D. Meier, M. Fiebig, Magnetoelectric domain control in multiferroic $TbMnO_3$, Science 348 (2015) 1112–1115.
[7] C.-M. Chang, B. Mani, S. Lisenkov, I. Ponomareva, Thermally mediated mechanism to enhance magnetoelectric coupling in multiferroics, Phys. Rev. Lett. 114 (2015) 177205.
[8] T.E. Quickel, L.T. Schelhas, R.A. Farrell, N. Petkov, V.H. Le, S.H. Tolbert, Mesoporous bismuth ferrite with amplified magnetoelectric coupling and electric field-induced ferrimagnetism, Nat. Commun. 6 (2015).
[9] V. Verma, A. Beniwal, A. Ohlan, R. Tripathi, Structural, magnetic and ferroelectric properties of Pr doped multiferroics bismuth ferrites, J. Magn. Magn. Mater. 394 (2015) 385–390.
[10] R.V. Chopdekar, M. Buzzi, C. Jenkins, E. Arenholz, F. Nolting, Y. Takamura, Giant reversible anisotropy changes at room temperature in a (La, Sr) MnO3/Pb (Mg, Nb, Ti) O3 magneto-electric heterostructure, Sci. Rep. 6 (2016) 27501.
[11] T. Walther, U. Straube, R. Köferstein, S.G. Ebbinghaus, Hysteretic magnetoelectric behavior of $CoFe_2O_4$–$BaTiO_3$ composites prepared by reductive sintering and reoxidation, J. Mater. Chem. C 4 (2016) 4792–4799.
[12] J.F. Scott, Room-temperature multiferroicmagnetoelectrics, NPG Asia Mater. 5 (2013) e72.
[13] W. Eerenstein, N. Mathur, J.F. Scott, Multiferroic and magnetoelectric materials, Nature 442 (2006) 759–765.
[14] Y. Wang, J. Hu, Y. Lin, C.-W. Nan, Multiferroic magnetoelectric composite nanostructures, NPG Asia Mater. 2 (2010) 61–68.
[15] C.T.M. Dung, N.H.T. Thi, K.H.T. Ta, V.C. Tran, B.T. Le Nguyen, Relaxor behaviors in $xBaTiO_3$–$(1-x)CoFe_2O_4$ materials, J. Magn. 20 (2015) 353–359.
[16] T. Woldu, B. Raneesh, M.R. Reddy, N. Kalarikkal, Grain size dependent magnetoelectric coupling of $BaTiO_3$ nanoparticles, RSC Adv. 6 (2016) 7886–7892.
[17] A. Singh, I. Choudhary, S. Mehta, S. Dahiya, C.S. Walia, K. Raina, R. Chatterjee, Optimal multiferroic properties and enhanced magnetoelectric coupling in $SmFeO_3$-$PbTiO_3$ solid solutions, J. Appl. Phys. 107 (2010) 084106.
[18] P. Pulišová, J. Kováč, A. Voigt, P. Raschman, Structure and magnetic properties of Co and Ni nano-ferrites prepared by a two-step direct microemulsions synthesis, J. Magn. Magn. Mater. 341 (2013) 93–99.
[19] F. Saffari, P. Kameli, M. Rahimi, H. Ahmadvand, H. Salamati, Effects of co-substitution on the structural and magnetic properties of $NiCo_xFe_{2-x}O_4$ ferrite nanoparticles, Ceram. Int. 41 (2015) 7352–7358.
[20] B. Xiao, Y. Dong, N. Ma, P. Du, Formation of sol–gel in situ derived BTO/NZFO composite ceramics with considerable dielectric and magnetic properties, J. Am. Ceram. Soc. 96 (2013) 1240–1247.
[21] S. Ojha, W.C. Nunes, N.M. Aimon, C.A. Ross, Magnetostatic interactions in self-assembled Co_xNi_{1-x} Fe_2O_4/$BiFeO_3$ multiferroic nanocomposites, ACS Nano 10 (2016) 7657–7664.
[22] H. Yang, G. Zhang, Y. Lin, Enhanced magnetoelectric properties of the laminated $BaTiO_3$/$CoFe_2O_4$ composites, J. Alloy. Compd. 644 (2015) 390–397.
[23] A. Chaudhuri, K. Mandal, Large magnetoelectric properties in $CoFe_2O_4$: $_{BaTiO3}$ core–shell nanocomposites, J. Magn. Magn. Mater. 377 (2015) 441–445.
[24] R.-F. Zhang, C.-Y. Deng, L. Ren, Z. Li, J.-P. Zhou, The giant dielectric constant and high initial permeability of $BaTiO_3$-$Ni_{0.5}Zn_{0.5}Fe_2O_4$ composite ceramics, ECS J. Solid State Sci. Technol. 2 (2013) N165–N168.
[25] D. Ghosh, A. Sakata, J. Carter, P.A. Thomas, H. Han, J.C. Nino, J.L. Jones, Domain wall displacement is the origin of superior permittivity and piezoelectricity in BaTiO3 at intermediate grain sizes, Adv. Funct. Mater. 24 (2014) 885–896.
[26] S. Lokare, R. Devan, B. Chougule, Structural analysis and electrical properties of ME composites, J. Alloy. Compd. 454 (2008) 471–475.
[27] Y. Lu, K. Sagara, Y. Matsuda, L. Hao, Y.R. Jin, H. Yoshida, Effect of Cu powder addition on thermoelectric properties of Cu/TiO_2– x composites, Ceram. Int. 39 (2013) 6689–6694.
[28] G. Arlt, D. Hennings, Dielectric properties of fine-grained barium titanate ceramics, J. Appl. Phys. 58 (1985) 1619–1625.
[29] G. Kwei, A. Lawson, S. Billinge, S. Cheong, Structures of the ferroelectric phases of barium titanate, J. Phys. Chem. 97 (1993) 2368–2377.
[30] A. Baji, Y.-W. Mai, R. Yimnirun, S. Unruan, Electrospun barium titanate/cobalt ferrite composite fibers with improved magnetoelectric performance, RSC Adv. 4 (2014) 55217–55223.
[31] M. Yashima, T. Hoshina, D. Ishimura, S. Kobayashi, W. Nakamura, T. Tsurumi, S. Wada, Size effect on the crystal structure of barium titanate nanoparticles, J. Appl. Phys. 98 (2005) 014313.
[32] X.-H. Wang, I.-W. Chen, X.-Y. Deng, Y.-D. Wang, L.-T. Li, New progress in development of ferroelectric and piezoelectric nanoceramics, J. Adv. Ceram. 4 (2015) 1–21.
[33] S. Ram, A. Jana, T. Kundu, Ferroelectric BaTiO3 phase of orthorhombic crystal structure contained in nanoparticles, J. Appl. Phys. 102 (2007) 4107.
[34] D. Ghosh, H. Han, J.C. Nino, G. Subhash, J.L. Jones, Synthesis of BaTiO3-20wt% $CoFe_2O_4$ nanocomposites via spark plasma sintering, J. Am. Ceram. Soc. 95 (2012) 2504–2509.
[35] A. Gupta, R. Chatterjee, Magnetic, dielectric, magnetoelectric, and microstructural studies demonstrating improved magnetoelectric sensitivity in three-phase $BaTiO_3$–$CoFe_2O_4$–poly (vinylidene-fluoride) composite, J. Appl. Phys. 106 (2009) 024110.
[36] A. Gupta, R. Chatterjee, Dielectric and magnetoelectric properties of $BaTiO_3$–$Co_{0.6}Zn_{0.4}Fe_{1.7}Mn_{0.3}O_4$ composite, J. Eur. Ceram. Soc. 33 (2013) 1017–1022.
[37] G.C. Montanari, P.H.F. Morshuis, Space charge phenomenology on polymeric insulating materials, IEEE Trans. Dielectr. Electr. Insul. 12 (2005) 754–767.
[38] F. Rogti, M. Ferhat, Maxwelle-Wagner polarization and interfacial charge at the multilayers of thermoplastic polymers, J. Electrost. 72 (2014) 91–97.
[39] Y. Tan, J. Zhang, Y. Wu, C. Wang, V. Koval, B. Shi, H. Ye, R. McKinnon, G. Viola, H. Yan, Unfolding grain size effects in barium titanate ferroelectric ceramics, Sci. Rep. 5 (2015).
[40] Y. Mao, S. Mao, Z.-G. Ye, Z. Xie, L. Zheng, Size-dependences of the dielectric and ferroelectric properties of $BaTiO_3$/polyvinylidene fluoride nanocomposites, J. Appl. Phys. 108 (2010) 4102.
[41] J. Scott, Ferroelectrics go bananas, J. Phys.: Condens. Matter 20 (2008) 021001.
[42] E. Akdogan, C. Rawn, W. Porter, E. Payzant, A. Safari, Size effects in $PbTiO_3$ nanocrystals: effect of particle size on spontaneous polarization and strains, J. Appl. Phys. 97 (2005) 084305.
[43] J. Adam, T. Lehnert, G. Klein, R.M. McMeeking, Ferroelectric properties of composites containing BaTiO3 nanoparticles of various sizes, Nanotechnology 25 (2014) 065704.
[44] H. Baaziz, A. Tozri, E. Dhahri, E. Hlil, Effect of particle size reduction on the structural, magnetic properties and the spin excitations in ferromagnetic insulator $La_{0.9}$ $Sr_{0.1}$ MnO_3 nanoparticles, Ceram. Int. 41 (2015) 2955–2962.
[45] R. Panda, R. Muduli, D. Behera, Electric and magnetic properties of Bi substituted cobalt ferrite nanoparticles: evolution of grain effect, J. Alloy. Compd. 634 (2015) 239–245.
[46] P. Pahuja, R. Sharma, V. Singh, R.P. Tandon, Novel method of synthesis of multiferroic nickel cobalt ferrite–barium strontium titanate composite system, Int. J. Appl. Ceram. Technol. 12 (2015).

Ceramics International xxx (xxxx) xxx–xxx

Contents lists available at ScienceDirect

Ceramics International

journal homepage: www.elsevier.com/locate/ceramint

$PbTiO_3$–$Ni_{0.5}Co_{0.5}Fe_2O_4$ multiferroic nanocomposites: Impact of ball-milling on dielectric, magnetic and ferroelectric properties

Sushma Lather[a], Jasvir Dalal[a], Anjli Gupta[a], Sukhbir Singh[b], D.P. Singh[c], Sajjan Dahiya[a], A.S. Maan[a], Rahul Tripathi[b,d,*], Anil Ohlan[a,**]

[a] Department of Physics, Maharshi Dayanand University, Rohtak 124001, India
[b] University Institute of Engineering and Technology, Maharshi Dayanand University, Rohtak 124001, India
[c] Department of Physics, Thapar University, Patiala 147004, India
[d] Department of Physics, Chaudhary Bansi Lal University, Bhiwani 127021, India

ARTICLE INFO

Keywords:
Multiferroics
Ball milling
Nanocomposites
Magnetic properties
Dielectric properties

ABSTRACT

The structural, dielectric, ferroelectric and magnetoelectric (ME) properties of multiferroic [$PbTiO_3$-$Ni_{0.5}Co_{0.5}Fe_2O_4$] (PT-NCF) composites have been discussed at room temperature. The uniformly distributed two-phase composites of $PbTiO_3$ (ferroelectric) dispersed into nano-sized $Ni_{0.5}Co_{0.5}Fe_2O_4$ (ferromagnetic) of different particle size were synthesized by employing high energy ball milling for 12, 24 and 48 h respectively. The phase and morphology of composites were confirmed by XRD and SEM analysis respectively. The dielectric properties were determined at different frequencies (i.e. from 1 kHz to 1 MHz) and it is observed that the dielectric constant and ferroelectric transition temperature (T_C) decreases with particle size. Further, the ferroelectric behavior of the composites was discussed at room temperature by examining the P-E loops. The magnetic and magnetoelectric measurements were performed to analyze the effect of particle size on ferromagnetic and magnetoelectric properties of PT-NCF composites. The coexistence of ferroelectric and ferromagnetic properties in composites with strong ME coupling is essential for a good multiferroic composites material and its applications.

1. Introduction

The coexistence of ferroelectricity and ferromagnetism in a single compound along with a strong coupling between them is the basic requirement of multiferroic materials [1–4]. Practically, the multiferroic properties can be achieved either in a single phase where two or more ferroic orders (like ferromagnetic and ferroelectric etc.) co-exist or in a form of composites, where two or more phases combine to form a multifunctional composites i.e. each individual order associated with corresponding phase would act together to form a multiferroic composite [5–9]. Generally, it is observed that, these ferroic orders like ferromagnetic and ferroelectricity are mutually exclusive and a strong magnetoelectric (ME) coupling between them together in a single phase is difficult to obtain. However, these multiphase composites as stated above have much larger reported ME coupling in comparison with that of a single phase multiferroic material [10–13]. Therefore, a composite/ multilayer of ferroelectric and ferromagnetic phases/ layers serve as a better option to obtain strong ME coupling at room temperature. These multifunctional composites can preside over single phase material as they are easy to synthesis and can have a strong coupling at room temperature. Among these multiferroic composites, a composite with ferroelectric phase such as $BaTiO_3$ or $PbTiO_3$ and ferromagnetic phase like $CoFe_2O_4$ were extensively studied [14–17]. For instance, Zhang et al. [17] had studied the multiferroic properties of $Ni_{0.5}Zn_{0.5}Fe_2O_4$-Pb$(Zr_{0.53}Ti_{0.47})O_3$ whereas Pradhan et al. [18] have studied the effect of concentration for composites {(1-x)$Pb(Fe_{0.5}Nb_{0.5})O_3$-x$Ni_{0.65}Zn_{0.35}Fe_2O_4$}by taking x = 0.1,0.2,.03, 0.4. The latter, in their findings suggest that at x = 0.2, composite was found to be a good multiferroic material at room temperature. Motivated by these studies, $PbTiO_3$(PT)-$Ni_{0.5}Co_{0.5}Fe_2O_4$ (NCF) composite in 80:20 ratio was synthesized and effect of mechanical milling or particle size reduction on structural, dielectric, ferroelectric, magnetoelectric and magnetic properties were analyzed and discussed. The samples of $PbTiO_3$ (PT) were prepared by conventional solid state reaction route while that of $Ni_{0.5}Co_{0.5}Fe_2O_4$ (NCF) by sol-gel wet chemical method. The reduction in particle size of the composite was achieved by high energy ball-milling. All the ball-milled samples of PT-NCF are in submicron range and are systematically discussed by taking into account the effect of

* Corresponding author at: University Institute of Engineering and Technology, Maharshi Dayanand University, Rohtak 124001, India.
** Corresponding author.
E-mail addresses: rtrnpl@gmail.com, rahultripathi.phy@cblu.ac.in (R. Tripathi), anilohlan@gmail.com, anilohlan.physics@mdurohtak.ac.in (A. Ohlan).

https://doi.org/10.1016/j.ceramint.2018.11.195
Received 30 June 2018; Received in revised form 22 November 2018; Accepted 23 November 2018

particle size on various physical properties of $PbTiO_3$-$Ni_{0.5}Co_{0.5}Fe_2O_4$ nanocomposites.

2. Experimental

The nano-sized $Ni_{0.5}Co_{0.5}Fe_2O_4$ (NCF) ferromagnetic powder is prepared by conventional sol-gel precursor chemical process from Ni $(NO_3)_2{\cdot}6H_2O$, $Co(NO_3)_2{\cdot}6H_2O$ and $Fe(NO_3)_3{\cdot}9H_2O$. All nitrates (99.9% purity) were taken in stoichiometric ratio and were dissolved in distilled water (in molar ratio 0.5:0.5:2) to form a homogenous solution. Followed by the addition of citric acid, the solution was then heated at 80–90 °C with constant stirring for 2 h and pH of the solution was maintained by adding ammonia drop wise. Subsequently, the temperature of solution was raised to 100 °C with continuously stirring to form a viscous gel. Next, the gel was burnt to form a dendrite structure which was then ground for at least 30 min in pestle mortar. The precursor was calcined at 1100 °C for 2 h to form nickel cobalt ferrite.

The $PbTiO_3$ ferroelectric powder was synthesized by solid–state reaction method, by taking PbO (99.9%) and TiO_2 (99.9%) in an appropriate ratio and ball-milled for 4 h. The homogeneous mixture was then calcined at 900 °C for 2 h to get $PbTiO_3$.

As per the previous studies reported in the literature, composites of ferroelectric (PT) and ferromagnetic (NCF) powders were obtained by mixing them in a mass ratio of 80:20 respectively in a high energy ball mill for different durations i.e. 12, 24 and 48 h. Depending upon the grinding duration, these nanocomposites powder of $PbTiO_3 - Ni_{0.5}Co_{0.5}Fe_2O_4$ were named as PT-NCF0, PT-NCF1, PT-NCF2 and PT-NCF3 for 0 (mixed using pestle mortar for 2 h), 12, 24 and 48 h respectively. The detailed synthesis process is described in Fig. 1.

Further, the pellets of these composites were prepared by mixing PVA (polyvinyl alcohol) and applying a uni-axial pressure of 10 t using hydraulic press. Finally, the sintering of all samples was carried out at 850 °C for 2 h to form the fully dense nanocomposites ceramics. High temperature and longer sintering durations were avoided to maintain the grain size of the composites as well as to control the volatility of Pb associated with $PbTiO_3$. The phase purity of the PT-NCF composites was investigated by X-ray Diffractometer (XRD) with CuK_α radiation (Rigaku Miniflex - II, 600). The grain structure and morphology was studied by using scanning electron microscope (SEM) (su8010, Hitachi). The dielectric constant/ loss versus temperature profiles at 1 kHz and dielectric constant/ loss profiles at room temperature were taken by using the multifunctional impedance analyzer (Wayne-Kerr

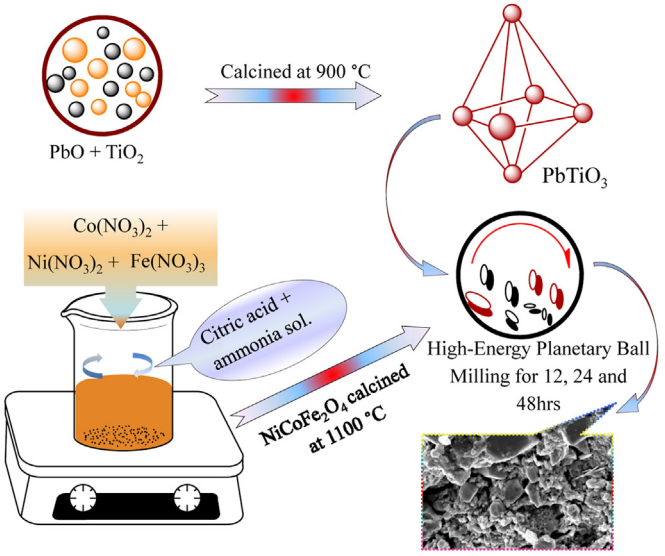

Fig. 1. Schematic illustration of synthesis process of $PbTiO_3$-$Ni_{0.5}Co_{0.5}Fe_2O_4$ nanocomposites.

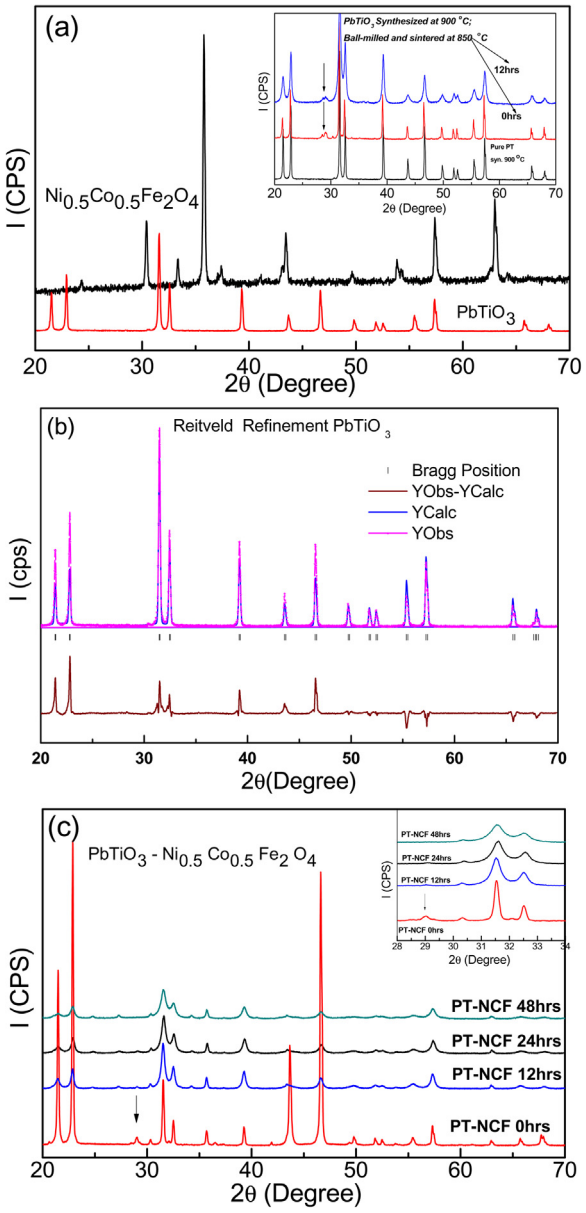

Fig. 2. (a) X-ray diffraction pattern of $PbTiO_3$, $NiCoFe_2O_4$; Inset shows a comparative XRD pattern of $PbTiO_3$ synthesized at 900 °C, ball-milled for 0 h and 12 h i.e. PT 0 h and PT 12 h sample finally sintered at 850 °C. (b) Reitveld refinement of pure $PbTiO_3$. (c) X-ray diffraction pattern of ball milled (0, 12, 24 and 48 h) PT-NCF composites; inset shows enlarged view between 2θ = 28–34°.

6500B) in a range from 100 Hz to10 MHz. Ferroelectric measurements were performed by using P-E loop tracer (Marine India ltd). Magnetic measurements were investigated using Variable Sample Magnetometer (VSM) and magneto electric coupling measurements were performed ME set up (Marine India Ltd).

3. Result and discussion

Fig. 2(a) shows the XRD pattern of the pure $PbTiO_3$ (PT), $Ni_{0.5}Co_{0.5}Fe_2O_4$ (NCF) synthesized at 900 and 1100 °C respectively. No impurity peak seems evident for PT phase, the NCF phase appears to crystallize in a cubic inverse spinal structure (JCPS card no.74–2081) [16]. In order to ascertain the lattice parameters of $PbTiO_3$, Reitveld refinement of pure $PbTiO_3$ was performed by taking tetragonal structure, as represented in Fig. 2(b). The c/a ratio as calculated from these refined parameters comes out to be 1.064 (a = 3.9002 Å; c = 4.151 Å)

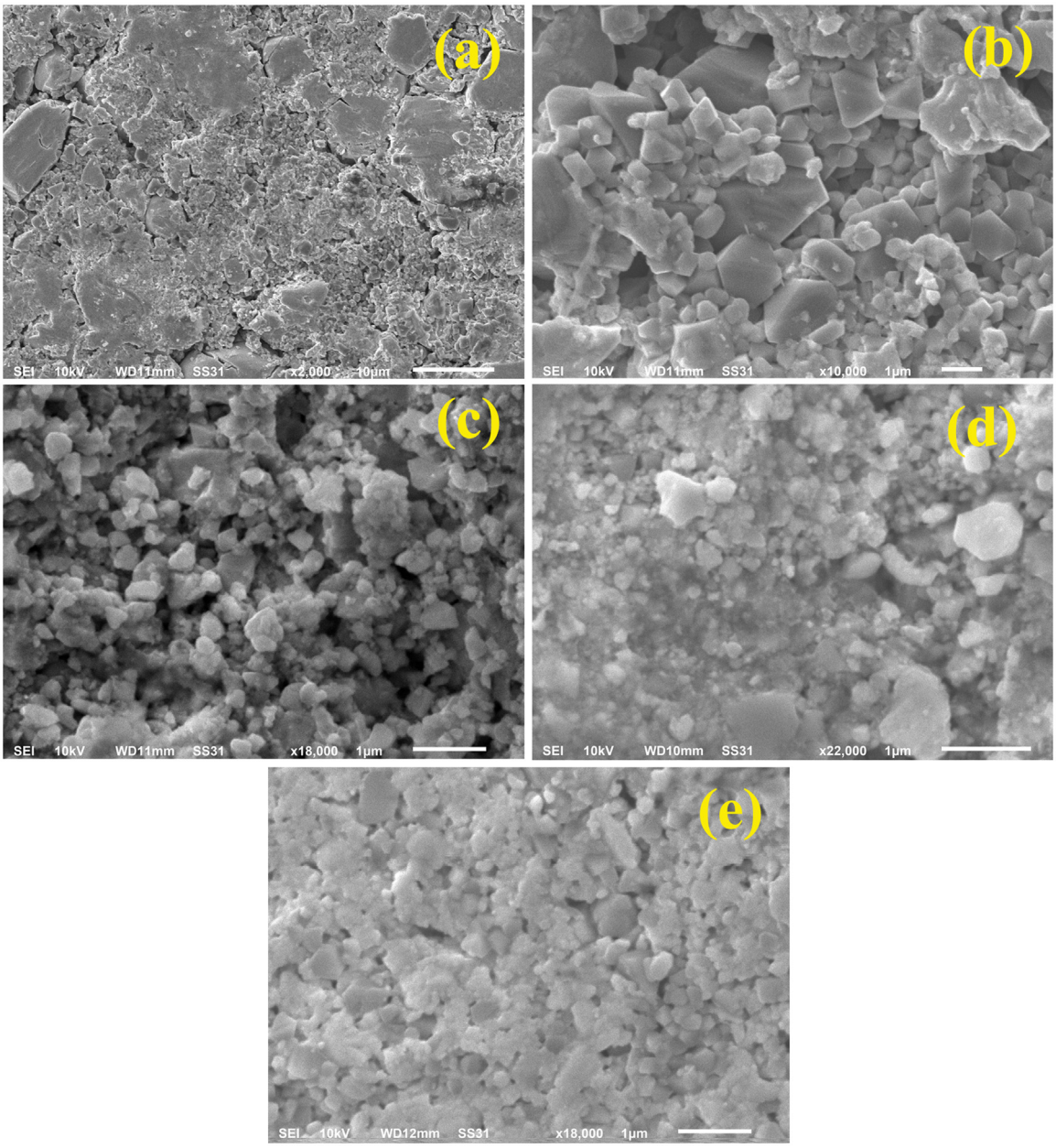

Fig. 3. SEM micrograph of (a)-(b) PT-NCF0, (c) PT-NCF1, (d) PT-NCF2 and (e) PT-NCF3.

which is very much same as reported earlier [19,20]. Hence, the tetragonality which is a crucial point for ferroelectric phase seems to have obtained in the present case.

Further, the core issue under investigation is to analyze the effect of particle size on the physical properties of the composite. Therefore, highly homogeneous composites were obtained by mixing PT-NCF in a planetary ball-mill, different particle sizes were obtained by varying the duration of milling and subsequently composite were sintered at 850 °C for 2 h to obtain dense samples. It is of immense significance at this point to mention that the PT phase used to prepare the composites has already been calcined at 900 °C and NCF at 1100 °C before ball-milling, followed by sintering at 850 °C for 2 h. It has been a widely known fact that the ceramics sintered at high temperature for longer duration followed by natural cooling have larger grain size in comparison with that of low temperature synthesis techniques. Patankar et al. [21] in their studies on $CuFe_2O_4$-$Ba_{0.8}Pb_{0.2}TiO_3$ has pointed out that the lower sintering temperature and shorter holding time helps in minimizing the Pb deficiency due to its volatility in $Ba_{0.8}Pb_{0.2}TiO_3$. Therefore, the procedure adopted above i.e. low sintering temperature less holding time ($T < 900$ °C; 2 h) may maintain both the grain size and Pb deficiency.

Fig. 2(c) shows the XRD pattern of composites under investigation. Interestingly, the composite without ball-milling i.e. PT-NCF0, exhibits enhanced peak intensity at $2\theta = 21.4$, 22.72, 43.7 and 46.49° (marked as *) corresponds to PT phase, whereas, such feature is absent in the XRD patterns of rest of the samples. On comparing PT-NCF0, 1, 2 and 3, it is observed that the intensity of XRD peaks decreases and peak width increase as the milling duration increases. It is a well-established fact that as the crystallite size decreases, the FWHM or peak width increase and intensity decreases, the samples under examination has exhibited the same trend (inset of Fig. 2(c)). Further, the synthesis parameters (except milling duration) for PT-NCF composites remain same and an impurity peak corresponds to secondary phase is observed (as indicated by an arrow) for all the samples. Moreover, the composite PT-NCF0 was sintered at 850 °C without ball-milling (0 h). Therefore, this impurity peak may have aroused due to evaporation of Pb which might have

occurred after mixing of PT and NCF phases followed by sintering and thus led to formation of secondary phase. Consequently, no additional phase seems to evolve due to milling.

The average crystallite size of PT phase as calculated by Scherrer's formula from PT-NCF0, PT-NCF1, PT-NCF2, and PT-NCF3 are 54, 19, 18 and 11 nm respectively. Similarly, for NCF phase are 45, 43, 42 and 41 nm respectively. It is also pointed out here that the quality of particle size cannot be ascertained by Scherrer's calculations. Ishikawaet et al. [22,23] has reported an interesting fact in this regard, according to these authors the c/a ratio decrease with particle size and may be correlated with the shift in transition temperature (discussed later). In present case, the c/a ratio of PT phase (as in PT-NCF composite) with milling was not discussed in detail, but it is observed from Reitveld refinements that c/a ratio remains nearly the same for PT phase in these composites.

Moreover, during refinement of X-ray diffraction pattern, the number of open parameters were limited. Therefore, variation of c/a ratio in these composites may be discussed in detail and may form a part of another investigation. Now, in order to differentiate the effect of particle size and of sintering at 850 °C of composites, a separate study was performed on PT phase alone. Where pristine $PbTiO_3$ samples were synthesized by following the same route as mentioned in the experimental section, followed by ball-milling of 12 h and subsequently sintered it at 850 °C for 2 h to produce PT 0 h and PT 12 h. Further, on comparing the XRD data as obtained (inset of Fig. 2(a)), it is observed that there was no shift in the position of XRD peaks with milling, only width and intensity of the peak changes which can be explained on the basis of crystallite size. Moreover, similar impurity peaks as mentioned above for composites (marked with arrow) seems to occur for both the samples which further confirms the fact that impurity may have its origin in volatility of Pb.

The surface morphologies of the PT-NCF composites were studied by using Scanning Electron Microscopy (SEM). It is clearly evident from the surface profile of PT-NCF0 (Fig. 3(a and b)) that a homogeneous composite consists of two different phases co-exists, one with clear and larger grains while the other without clear grain boundaries at the same magnification. Therefore, it may be correlated that these dissimilar grain morphologies correspond to PT and NCF phases of the composite. On comparing the SEM micrographs of other composites, it was observed that the ball-milled samples were having smaller grain size with no clear grain boundaries. In other words, the average grain size of composite PT-NCF0 is large as compared with other composites i.e. PT-NCF1, PT-NCF2, PT-NCF3. Further, it is nearly difficult to calculate the grain size and analyze the effect of milling duration on the size of the composites grains with current resolution constraint. But it can be clearly observed that the milling has reduced the grain to a greater extent and enhanced the homogeneity of the mixer. The same fact may also be linked with the peak broadening of the XRD pattern. Moreover, on calculating the density of the samples by employing the Archimedes principle, it was found that the density of the composites has slightly increased for milled samples i.e. these samples has high sample density as compared with that of PT-NCF0. The corresponding values are 6.78 (PT-NCF0), 6.88 (12 h)· 6.87 (24 h) and 6.9 g/cm^3 (48 h).

The variation of dielectric constant and dielectric loss with temperature are shown in Fig. 4. The dielectric constant is calculated by the given equation,

$$K = (C_p \times t)/(A \in_0) \quad (1)$$

here Cp is capacitance, t is thickness of pellet, A is area of cross-section, and $\in_o$ is permittivity of free space. The significant changes were observed in the dielectric properties of PT-NCF composites with milling duration/particle size. The dielectric measurement with temperature was recorded at a given frequency of 1 kHz, as shown in Fig. 4(a). From these curves, it is clear that the value of the temperature where maximum dielectric constant occurs i.e. Ferroelectric transition temperature (T_c), decreases as the particle size decreases. In short, samples with higher milling duration have lower T_c. The occurrence of maxima for the dielectric constant with temperature in these composites has its origin in paraelectric-ferroelectric phase transition associated with $PbTiO_3$. Similar observations were reported by Mudinepalli et al. [24] for nanostructure $Ba_{0.8}Sr_{0.2}TiO_2$ ceramics and few others [20,22,23,25,26]. The values of dielectric constant and transition temperature for all samples are listed in Table 1. Interestingly, the change in the T_c as observed from Fig. 4(a) is more than 100 °C between PT-NCF2 and PT-NCF0 samples. The 48 h milled composites exhibits a diffused peak. The variation in dielectric properties may be understood by considering three factors: (a) particle size reduction of ferroelectric phase, (b) formation of composite in 80:20 ratio and (c) sintering of lead composites at 850 °C after calcinations at 900 °C for 2 h.

Several authors [20,22,23,26] have pointed out that with reduction in the particle size of $PbTiO_3$, the T_c, which corresponds to paraelectric-ferroelectric transition temperature shifted to lower side and the reason for such behavior was attributed to the decrease in c/a ratio i.e tetragonality of $PbTiO_3$ structures decreases, which is responsible for ferroelectric phase. But, in the current study, though the refinement of XRD pattern was performed by taking two phases with limited parameters and no reportable variation in c/a ratio was observed for nanocomposites of PT-NCF. In order to ascertain the reason for shift in T_c of composites, the dielectric properties of pristine $PbTiO_3$ (single phase) was carried out. Here, the pristine $PbTiO_3$ were milled for 0 h and 12 h and the XRD pattern of the same was mentioned in the XRD discussions above i.e. PT 0 h and PT 12 h. The inset of Fig. 4(a), shows the dielectric constant as a function of temperature, the variation in T_c for PT 0 h and PT 12 h was recorded and it is observed that the T_c varies with milling duration/ particle size and changes about 20 °C which is in accordance with some earlier reports [20,22,23]. Further, as far as reduction in T_c due to point (b) above is concerned, Patankar et al. [21] in their paper has pointed out the ratio of ferroelectric and ferromagnetic phase plays an important role in analyzing the dielectric behavior of a composite. The dielectric behavior of such composites systems may be discussed by considering the Fe^{2+}-Fe^{3+} exchange interactions suggesting that the polarization in these compositions is similar to that of conduction process in ferrites. However, in the composites under study, conductivity of PT-NCF3 has increased in comparison with that of PT-NCF0. Moreover, the factor mentioned at point (c) which directly linked with the volatility of lead during formation of $PbTiO_3$. In this connection, Forrester et al. [19] and Chaudhari et al. [27] has mentioned that volatility increases with high temperature and longer duration sintering. In the light of the above, keeping in mind point (b) and (c), it is stated that all the composites of PT and NCF, were formed by mixing ferromagnetic and ferroelectric phase in a fixed ratio sintered at lower temperature for shorter duration, still the observed change in the transition temperature (Fig. 4(a)) is more than 100 °C between PT-NCF0 and PT-NCF2. To further confirm our observation, composites PT-NCF0, PT-NCF1 and PT-NCF3 were synthesized again under similar conditions and it was found that T_c again varies more than 100 °C for PT-NCF3 which is a significant change. It is worth mentioning that even though in successive trial the exact values of transition temperature did not exactly match with the composites under study but one thing is certain that the transition temperature varies with ball-milling/ particle size and hence, reflecting the fact that milling has reduced the particle size. Therefore, the particle size and presence of ferromagnetic phase together may be responsible for such a large variation in T_c. Nevertheless the effect of volatility of lead may not be totally ruled out.

The dielectric losses as a function of temperature are shown in Fig. 4(b). It is observed from these plots that at lower temperatures, curves all the samples coincide, dielectric loss increases at higher temperatures.

The dielectric behaviors of all composites with frequency were recorded in a range from 1 kHz to 1 MHz at room temperature, as shown in Fig. 5. From these curves, it is observed that the dielectric constant decreases with frequency. Generally, at low frequency high values may

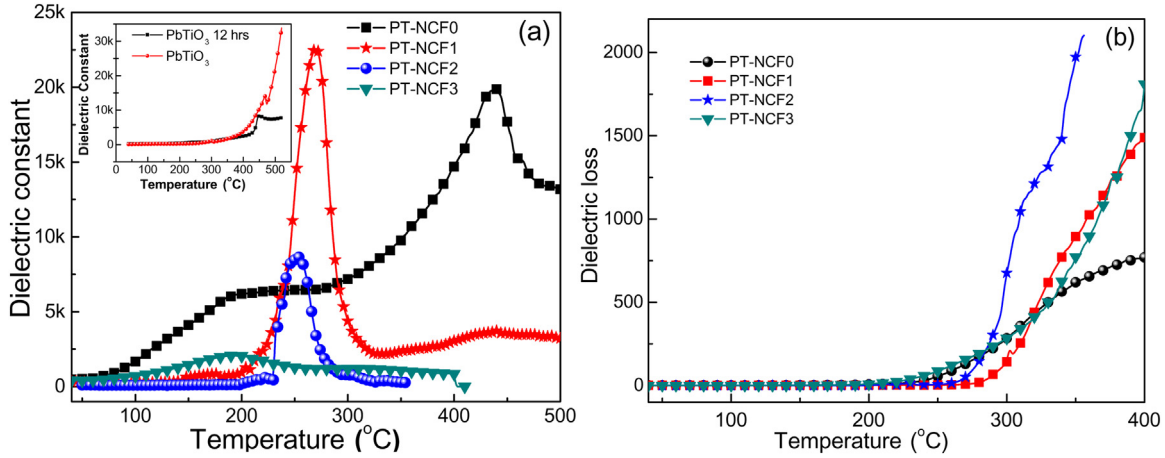

Fig. 4. (a)Variation of dielectric constant whereas inset shows the variation of dielectric constant of pure $PbTiO_3$ (PT 0 h) and 12 h milled $PbTiO_3$ sintered at 850 °C and (b) change in dielectric loss behavior with temperature.

Table 1
Values of transition temperature, dielectric constant and dielectric losses of PT-NCF.

Property	PT-NCF0	PT-NCF1	PT-NCF2	PT-NCF3
Ferroelectric T_c (°C)	438	270	254	–
Dielectric loss at T_c (°C)	886	6.8	6.5	3.8
Dielectric constant at T_C (°C)	20,000	22,000	8500	2000

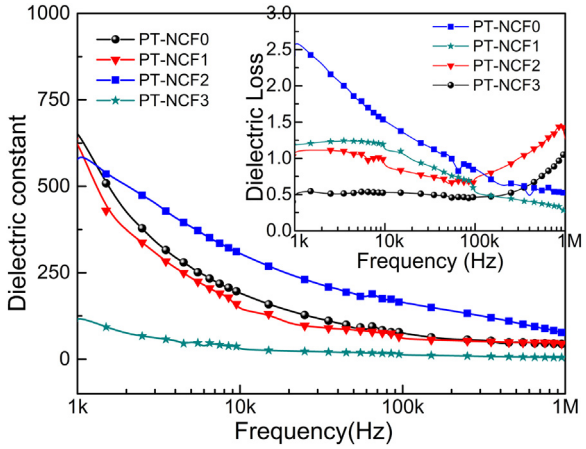

Fig. 5. Variation of dielectric constant with frequency at room temperature whereas the inset shows dielectric loss as a function of frequency at room temperature.

Table 2
Values of dielectric constant and dielectric losses at 1 kHz for PT-NCF at room temperature.

Property	PT-NCF0	PT-NCF1	PT-NCF2	PT-NCF3
Dielectric loss at 1 kHz	2.6	1.2	1.0	0.5
Dielectric constant at 1 kHz	660	629	604	124

be correlated with Maxwell–Wagner interfacial polarization [28]. The values of dielectric constant at lower frequencies remain close except for PT-NCF3. The inset to Fig. 5 shows the dielectric losses [29], at lower frequencies the losses were less for milled composites. Table 2 shows the value of dielectric constant and dielectric losses at 1 kHz for PT-NCF at room temperature.

The P-E (Polarization vs. Electric field) loops of all the composites

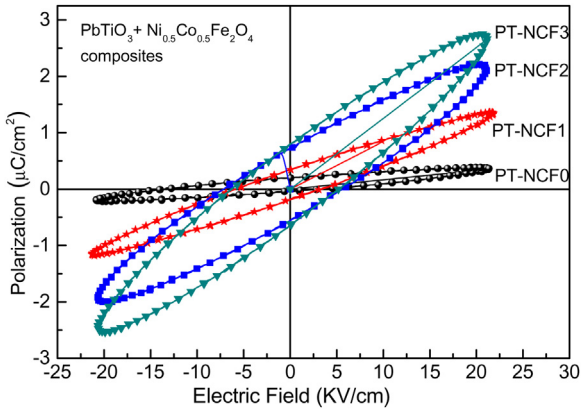

Fig. 6. Ferroelectric (P-E) hysteresis loops for composites PT-NCF at room temperature.

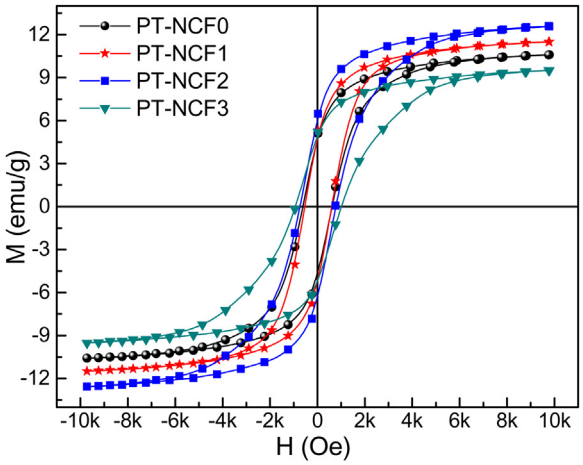

Fig. 7. M-H plots of $PbTiO_3$-$Ni_{0.5}Co_{0.5}Fe_2O_4$ composites.

with different grain size/ milling duration obtained at room temperature are shown in Fig. 6. The normal sigmoid shape is not observed and loops seem lossy in nature. The area of the loop increases with decrease in the particle size. In case of $BaTiO_3$ [30], size greater than the critical size is required for enhanced/optimized dielectric and ferroelectric properties. It is evident from XRD and SEM studies that average grain size in these milled composites is in submicron range, therefore, superior ferroelectric properties were not achieved, as apparent from

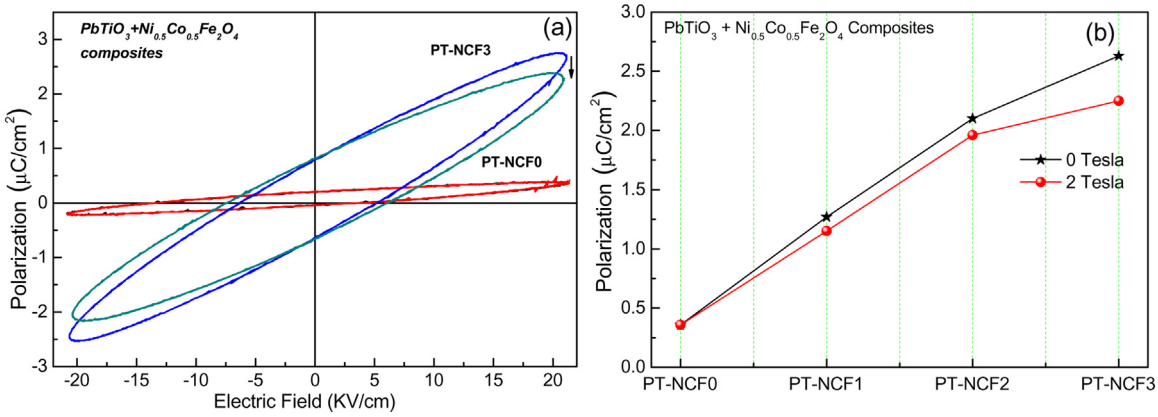

Fig. 8. (a) P-E loop with (H= 2Tesla) and without magnetic field of $PbTiO_3$-$Ni_{0.5}Co_{0.5}Fe_2O_4$ 0 h and 48 h ball-milled composites. (b) Effect of magnetization on Polarization of $PbTiO_3$-$Ni_{0.5}Co_{0.5}Fe_2O_4$ composites at E = 20.8 kV/cm.

Fig. 6. Though the condition of saturation polarization was not apparent in present case [31], but the magnitude of remnant polarization (P_r) as obtained from the P-E loops suggest that P_r increase, i.e.Pr = 0.2, 0.34, 0.71, 0.79 μC/cm^2 for milled samples i.e. PT-NCF3 has the highest value. Moreover, magnitude of coercive field has maximum value for PT-NCF0 i.e. E_c = 12.2 kV/cm for PT-NCF0 composite.

Magnetization verses magnetic field M-H curves are shown in Fig. 7. The samples were placed in a magnetic field that varies upto10 KOe. The percentage of NCF phase is small in comparison with that of PT phase but still the magnetization values obtained for all the composites were substantial good [32–34]. The values of saturation magnetization i.e. M_s = 10.55, 11.48, 12.61 and 9.48 emu/g for PT-NCF0, PT-NCF1, PT-NCF2 and PT-NCF3 composites respectively, retentivity remains almost same for all the samples except for PT-NCF2. Further, the coercive field, Hc = 618, 532, 732 and 918 Oe for PT-NCF 0, 12, 24 and 48 h respectively.

The measurement of magnetoelectric (ME) coupling of the composites PT-NCF0, PT-NCF1, PT-NCF2 and PT-NCF3 was carried out by (i) measuring magnetoelectric coupling coefficient (α_E), which measures the voltage induced in the sample under the influence of static magnetic field, superimposed with a small ac field and indirectly by (ii) measuring change in the P-E curves with and without magnetic field. No substantial indication of ME coupling was obtained by employing former method, therefore, results of indirect method of ME effect were plotted; plots are shown in Fig. 8(a). It is clearly observed from Fig. 8(a) that the P-E loop of PT-NCF0 remained unaffected under magnetic field of 2 T. However, variations in the P-E loops were observed for all other composites. In order to analyze it further, variations in polarization was plotted for different samples and are shown in Fig. 8(b). Even though it is quite evident from these plots that the absolute change is small but the strength of ME coupling seems to enhance in composite under examinations with reduction in particle size.

4. Conclusion

The multiferroic composite of $PbTiO_3$-$Ni_{0.5}Co_{0.5}Fe_2O_4$ was ball-milled to produce composites of submicron range. The effect of size reduction was clearly visible in X-ray diffraction patterns, SEM micrographs and dielectric measurements. In dielectric measurements, a large variation in the transition temperature, T_c, was recorded which may be correlated with particle size and the presence of ferroelectric phase. The ME coupling in PT-NCF seems weak but can be enhanced with optimized ferroelectric grain size (critical size) and proper ratio of ferromagnetic phase.

Acknowledgement

The authors are thankful to Department of Science and Technology, New Delhi, India and University Grants Commission, New Delhi, India for providing financial support under DST-FIST (SR/FST/PSI-162/2011) and UGC-SAP (F530/5/DRS/2012(SAP-1)) schemes, respectively. One of the authors RT would like to thank UGC-India for providing financial help under UGC-MRP (F. No. 43–402/2014(SR)). We would like to acknowledge Marine India for providing facility of P-E under magnetic field.

References

[1] S. Dong, J.-M. Liu, S.-W. Cheong, Z. Ren, Multiferroic materials and magnetoelectric physics: symmetry, entanglement, excitation, and topology, Adv. Phys. 64 (2015) 519–626.
[2] Y. Han, Z. Zhang, F. Wang, W. Mi, K. Zhang, Fabrication and characterization of a magnetoelectric memory cell of $50Ba(Zr_{0.2}Ti_{0.8})O_3$-$50Ba_{0.7}Ca_{0.3}TiO_3/Fe_{70}Ga_{30}$, Mater. Lett. 170 (2016) 192–195.
[3] Z. Zhou, B.M. Howe, M. Liu, T. Nan, X. Chen, K. Mahalingam, N.X. Sun, G.J. Brown, Interfacial charge-mediated non-volatile magnetoelectric coupling in $Co_{0.3}Fe_{0.7}$/$Ba_{0.6}Sr_{0.4}$ TiO_3/Nb: $SrTiO_3$ multiferroic heterostructures, Sci. Rep. 5 (2015) 7740.
[4] S.-W. Cheong, M. Mostovoy, Multiferroics: a magnetic twist for ferroelectricity, Nat. Mater. 6 (2007) 13.
[5] S. Ravi, C. Senthil kumar, Room temperature multiferroicity in a new Ba_2FeMnO_6 double perovskite material, Ceram. Int. 43 (2017) 14441–14445.
[6] M. Matsubara, S. Manz, M. Mochizuki, T. Kubacka, A. Iyama, N. Aliouane, T. Kimura, S.L. Johnson, D. Meier, M. Fiebig, Magnetoelectric domain control in multiferroic $TbMnO_3$, Science 348 (2015) 1112–1115.
[7] C.-M. Chang, B. Mani, S. Lisenkov, I. Ponomareva, Thermally mediated mechanism to enhance magnetoelectric coupling in multiferroics, Phys. Rev. Lett. 114 (2015) 177205.
[8] T.E. Quickel, L.T. Schelhas, R.A. Farrell, N. Petkov, V.H. Le, S.H. Tolbert, Mesoporous bismuth ferrite with amplified magnetoelectric coupling and electric field-induced ferrimagnetism, Nat. Commun. 6 (2015) 6562.
[9] V. Verma, A. Beniwal, A. Ohlan, R. Tripathi, Structural, magnetic and ferroelectric properties of Pr doped multiferroics bismuth ferrites, J. Magn. Magn. Mater. 394 (2015) 385–390.
[10] R.V. Chopdekar, M. Buzzi, C. Jenkins, E. Arenholz, F. Nolting, Y. Takamura, Giant reversible anisotropy changes at room temperature in a (La, Sr) MnO_3/Pb (Mg, Nb, Ti) O_3 magneto-electric heterostructure, Sci. Rep. 6 (2016) 27501.
[11] T. Walther, U. Straube, R. Köferstein, S.G. Ebbinghaus, Hysteretic magnetoelectric behavior of $CoFe_2O_4$-$BaTiO_3$ composites prepared by reductive sintering and re-oxidation, J. Mater. Chem. C 4 (2016) 4792–4799.
[12] R. Rakhikrishna, J. Isaac, J. Philip, Magneto-electric coupling in multiferroic nanocomposites of the type $x(Na_{0.5}K_{0.5})_{0.94}Li_{0.06}NbO_3(1-x)CoFe_2O_4$: role of ferrite phase, Ceram. Int. 43 (2017) 664–671.
[13] S. Guo, B. Luo, H. Pei, C. Chen, K. Jin, Effect of space charge on dielectric and magneto-dielectric behaviors in $Ba_{0.85}Ca_{0.15}Zr_{0.1}Ti_{0.9}O_3$/ $La_{0.67}Sr_{0.33}MnO_3$ heterostructure, Ceram. Int. 44 (2018) 14286–14290.
[14] Y. Wang, J. Hu, Y. Lin, C.-W. Nan, Multiferroic magnetoelectric composite nanostructures, NPG Asia Mater. 2 (2010) 61.
[15] C.T.M. Dung, N.H.T. Thi, K.H.T. Ta, V.C. Tran, B.T. Le Nguyen, P.A. Do, A.T. Dang, H. Ju, B.T. Phan, Relaxor Behaviors in $xBaTiO_3$–(1-x) $CoFe_2O_4$ Materials, J. Magn. 20 (2015) 353–359.
[16] S. Lather, A. Gupta, J. Dalal, V. Verma, R. Tripathi, A. Ohlan, Effect of mechanical milling on structural, dielectric and magnetic properties of $BaTiO_3$–$Ni_{0.5}Co_{0.5}Fe_2O_4$ multiferroic nanocomposites, Ceram. Int. 43 (2017) 3246–3251.

[17] H. Zhang, S.W. Or, H.L.W. Chan, Multiferroic properties of Ni $_{0.5}$Zn $_{0.5}Fe_2O_4$-Pb$(Zr_{0.53}Ti_{0.47})O_3$ ceramic composites, J. Appl. Phys. 104 (2008) 104109.
[18] D.K. Pradhan, S.K. Barik, S. Sahoo, V.S. Puli, R. Katiyar, Investigations on electrical and magnetic properties of multiferroic[(1- x)$Pb(Fe_{0.5}Nb_{0.5})O_3$-x$Ni_{0.\ 65}Zn_{0.\ 35}Fe_2O_4$] composites, J. Appl. Phys. 113 (2013) 144104.
[19] J.S. Forrester, J.S. Zobec, D. Phelan, E.H. Kisi, Synthesis of $PbTiO_3$ ceramics using mechanical alloying and solid state sintering, J. Solid State Chem. 177 (2004) 3553–3559.
[20] S. Kim, Mc Jun, Sc Hwang, Preparation of undoped lead titanate ceramics via sol-gel processing, J. Am. Ceram. Soc. 82 (1999) 289–296.
[21] K. Patankar, V. Mathe, R. Mahajan, S. Patil, R.M. Reddy, K. Siva Kumar, Dielectric behaviour and magnetoelectric effect in $CuFe_2O_4$-$Ba_{0.8}Pb_{0.2}TiO_3$ composites, Mater. Chem. Phys. 72 (2001) 23–29.
[22] K. Ishikawa, K. Yoshikawa, N. Okada, Size effect on the ferroelectric phase transition in $PbTiO_3$ ultrafine particles, Phys. Rev. B 37 (1988) 5852.
[23] K. Ishikawa, T. Nomura, N. Okada, K. Takada, Size effect on the phase transition in $PbTiO_3$ fine particles, Jpn. J. Appl. Phys. 35 (1996) 5196.
[24] V.R. Mudinepalli, L. Feng, W.-C. Lin, B. Murty, Effect of grain size on dielectric and ferroelectric properties of nanostructured $Ba_{0.8}Sr_{0.2}TiO_3$ ceramics, J. Adv. Ceram. 4 (2015) 46–53.
[25] A. Singh, I. Choudhary, S. Mehta, S. Dahiya, C.S. Walia, K. Raina, R. Chatterjee, Optimal multiferroic properties and enhanced magnetoelectric coupling in $SmFeO_3$–$PbTiO_3$ solid solutions, J. Appl. Phys. 107 (2010) 084106.
[26] S. Chattopadhyay, P. Ayyub, V. Palkar, M. Multani, Size-induced diffuse phase transition in the nanocrystalline ferroelectric $PbTiO_3$, Phys. Rev. B 52 (1995) 13177.
[27] V.A. Chaudhari, G.K. Bichile, Synthesis, structural, and electrical properties of pure $PbTiO_3$ ferroelectric ceramics, Smart Mater. Res. 2013 (2013).
[28] K. Patankar, S. Joshi, B. Chougule, Dielectric behaviour in magnetoelectric composites, Phys. Lett. A 346 (2005) 337–341.
[29] P. Pahuja, R. Sharma, V. Singh, R.P. Tandon, Novel method of synthesis of multiferroic nickel cobalt ferrite–barium strontium titanate composite system, Int. J. Appl. Ceram. Technol. 12 (2015).
[30] Y. Tan, J. Zhang, Y. Wu, C. Wang, V. Koval, B. Shi, H. Ye, R. McKinnon, G. Viola, H. Yan, Unfolding grain size effects in barium titanate ferroelectric ceramics, Sci. Rep. 5 (2015) 9953.
[31] Y. Mao, S. Mao, Z.-G. Ye, Z. Xie, L. Zheng, Size-dependences of the dielectric and ferroelectric properties of $BaTiO_3$/ polyvinylidene fluoride nanocomposites, J. Appl. Phys. 108 (2010) 014102.
[32] R. Panda, R. Muduli, D. Behera, Electric and magnetic properties of Bi substituted cobalt ferrite nanoparticles: evolution of grain effect, J. Alloy. Compd. 634 (2015) 239–245.
[33] K. Torkar, O. Fredriksen, The effect of grain size on saturation magnetization of barium ferrite powders, Powder Metall. 2 (1959) 105–107.
[34] H. Baaziz, A. Tozri, E. Dhahri, E. Hlil, Effect of particle size reduction on the structural, magnetic properties and the spin excitations in ferromagnetic insulator $La_{0.9}Sr_{0.1}MnO_3$ nanoparticles, Ceram. Int. 41 (2015) 2955–2962.